TiO$_2$ and Reducing Gas: Intricate Relationships to Direct Reduction of Iron Oxide Pellets

PASQUALE CAVALIERE, BEHZAD SADEGHI, ALEKSANDRA LASKA, and DAMIAN KOSZELOW

In response to the imperative for sustainable iron production with reduced CO$_2$ emissions, this study delves into the intricate role of TiO$_2$ in the direct reduction of iron oxide pellets. The TiO$_2$-dependent reducibility of iron oxide pellets utilizing H$_2$ and CO gas across varied temperatures and gas compositions is thoroughly investigated. Our findings unveil the nuanced nature of the TiO$_2$ effect, underscored by its concentration-dependent behavior, revealing an optimal range between 1 and 1.5 pct TiO$_2$, where a neutral or positive impact on reduction kinetics and diffusion coefficient is observed. Notably, the synergistic interplay of CO and H$_2$ at 1000 °C emerges as particularly efficacious, suggesting complementary effects on the reduction process. The introduction of H$_2$ into the reducing atmosphere regulated by CO not only extends the transition range but also markedly expedites the rate of reduction. Furthermore, our study highlights the temperature sensitivity of the TiO$_2$ effect, with higher TiO$_2$ content correlating with prolonged reduction time in a 100 pct H$_2$ atmosphere at 900 °C. In a 100 pct H$_2$ atmosphere, the non-contributory role of TiO$_2$ stems from the water-gas shift reaction. Conversely, introducing H$_2$ into a CO-controlled reducing atmosphere with TiO$_2$ enhances the transition range and expedites the reduction rate. Additionally, our findings underscore the role of total iron content, revealing a direct correlation with the reduction process.

I. INTRODUCTION

AMONG the critical stages in iron and steel production, the reduction behavior of iron ore stands out as a pivotal process. The efficiency of this reduction process significantly impacts the overall productivity and sustainability of iron and steel manufacturing. The influence of oxide impurities, more precisely non-iron oxides, on the reducibility behavior of iron pellets has been a subject of considerable interest and research.[1–5] Each oxide plays a distinct role in shaping the kinetics and mechanisms of the reduction process. Comprehensive knowledge of the effects of individual oxides is imperative for steering the reduction process toward optimal

conditions, improving resource efficiency, and ultimately enhancing the efficiency of iron and steel production. Geological and climatic differences have caused a large amount of iron ore obtained in many quarries to have specific non-ferrous oxides impurities namely TiO$_2$, CaO, and SiO$_2$.[6,7] Meanwhile, the consequences of the presence of many of these oxides, except TiO$_2$, on the reducibility behavior of iron oxide pellets have been determined.[8,9] Numerous studies have been conducted to investigate the reducibility of iron oxide pellets with the presence of TiO$_2$, mostly focusing on the role of TiO$_2$ as a catalyst and less on the reduction kinetics and mechanisms. The findings have shown that incorporating TiO$_2$ into the pellet matrix enhances the reduction kinetics and improves the final reduction degree (the extent the reduction of iron oxide pellets).[2,10–12] The presence of TiO$_2$ promotes the formation of a more porous and reactive structure, leading to increased gas–solid interaction and a higher reduction rate. However, there is still debate regarding how TiO$_2$ affecting the reduction process, the optimal TiO$_2$ loading, and its influence on the mechanical properties and phase transformations of the pellets.[13,14]

The thermodynamic and kinetic aspects related to the TiO$_2$-dependent reducibility of iron oxide pellets were studied. Thermodynamic calculations and phase diagrams have been employed to predict the stability

PASQUALE CAVALIERE and BEHZAD SADEGHI are with the Department of Innovation Engineering, University of Salento, Via per Arnesano, 73100 Lecce, Italy. Contact e-mail: pasquale.cavaliere@unisalento.it ALEKSANDRA LASKA is with the Faculty of Mechanical Engineering and Ship Technology, Gdansk University of Technology, Narutowicza 11/12, 80-233, Gdansk, Poland. DAMIAN KOSZELOW is with the Advanced Materials Centre, Faculty of Electronics, Telecommunications and Informatics, Gdansk University of Technology, 80-233, Gdansk, Poland.
Manuscript submitted March 18, 2024; accepted June 4, 2024.

regions of various iron oxides and their mixtures with TiO$_2$ at different temperatures and gas compositions. Additionally, kinetic models have been developed to characterize the reduction reaction and estimate the rate constants. Paananen *et al.* presented a comprehensive thermodynamic analysis of the TiO$_2$-dependent reducibility of iron oxide pellets using H$_2$ and CO gas at high temperature.[11] The authors reported that the addition of TiO$_2$ to iron oxide pellets enhances their reducibility, leading to faster and more efficient reduction reactions. The presence of TiO$_2$ promotes the formation of intermediate phases, such as Fe3O4 and FeO, which facilitate the reduction process. The findings suggest that TiO$_2$ can be utilized as a catalyst to improve the reduction kinetics of iron oxide pellets. The presence of TiO$_2$ as a common non-ferrous oxide in the iron oxide pellets can effectively develop its potential as a catalyst to enhance the reduction process.[15–17] Studies show that TiO$_2$ can influence the reduction kinetics and phase transformation of iron oxides under different atmospheric conditions.[18,19] By changing the microstructural properties of the pellets, TiO$_2$ can enable faster reduction rates and improve the energy efficiency of the process, which is crucial for sustainable large-scale production.[11,20] Pimenta *et al.* focused on the kinetic modeling of the TiO$_2$-dependent reducibility of iron oxide pellets using H$_2$ and CO gas at high temperature.[21] The finding indicated that the kinetic behavior of the TiO$_2$-dependent reducibility of iron oxide pellets can be accurately described by the developed mathematical model. The results suggested that the kinetic model can be used to optimize the reduction process and improve the efficiency of iron oxide pellet production. It is demonstrated that the addition of TiO$_2$ to iron oxide pellets significantly affects the microstructure evolution during the reduction process.[21, 22]. TiO$_2$ promotes the formation of fine-grained structures and inhibits grain growth, which can also affect the mechanical properties of the reduced pellets.[23,24]

Studies have shown varying results, primarily due to different experimental conditions such as temperature, pellet composition, and gas atmosphere. In fact, the reducibility is improved by the addition of TiO$_2$ under high temperature conditions in a CO atmosphere,[11] while the effectiveness of TiO$_2$ may decrease at lower temperatures or in a predominantly H$_2$ atmosphere.[21,22] Additionally, in some studies, it was observed that TiO$_2$ contributes to the formation of a fine-grained microstructure that enables faster reduction rates, while other studies found that excessive TiO$_2$ loading could lead to the formation of stable complexes with iron oxides that hinder the reduction process. Various proposed mechanisms include the role of TiO$_2$ generating oxygen vacancies, facilitating electron transfer, and promoting the dissociation of H$_2$ and CO gases.[25] Some studies suggest that TiO$_2$ acts as a catalyst by donating electrons to the iron oxide lattice, while others propose its involvement in the formation of iron oxides with lower oxygen stoichiometry. TiO$_2$ can promote the reduction of Fe$_2$O$_3$ to Fe$_3$O$_4$ by increasing the surface mobility of oxygen vacancies.[26,27] In contrast, it suggested that TiO$_2$ may hinder the reduction

process by forming stable surface complexes with iron oxide species,[12,28,29] thereby reducing the availability of active sites for gas–solid reactions. Iron in the presence of TiO$_2$ can react quickly with the resulting holes and thus provide more electrons on the TiO$_2$ surface for the reduction process.[30] Further research is needed to conclusively determine the dominant mechanisms and their dependence on factors such as TiO$_2$ particle size and morphology.

Given that the presence of TiO$_2$ is a known impurity in the iron oxide pellets derived from geological resources and was not intentionally added to the pellets, it is critical to re-evaluate its impact on reduction kinetics and slag behavior in iron production.[7,21,31] While this study is primarily focused on elucidating the intricate relationships between naturally occurring TiO$_2$ and the direct reduction of iron oxide pellets, the recognition of its unintended presence emphasizes the importance of the findings in the context of industrial applications. Despite the challenges posed by TiO$_2$ contamination, this research sheds light on the impact on reduction kinetics in optimal concentration ranges. In addition, the flow characteristics affected by the presence of TiO$_2$ could influence the behavior of the slag, which could impact process efficiency and product quality.[17,23,32]

Despite the progress made, there are still several unresolved issues, such as the long-term stability of TiO$_2$-iron oxide systems, the scale-up of the production process, and the economical synthesis of TiO$_2$-modified pellets. Additionally, more comprehensive studies are needed to fully understand the mechanisms and kinetics involved in TiO$_2$-enhanced reduction. This study holds significant implications for understanding the nuanced role of TiO$_2$ in the reduction behavior of iron ore, particularly in the context of varying reducing atmospheres. By investigating the impact of TiO$_2$ on the reducibility and metallization of iron oxide pellets under different conditions, this research addresses key scientific questions surrounding the complex interactions between TiO$_2$ and reducing gases like H$_2$ and CO.

Previous studies on the role of TiO$_2$ in the direct reduction of iron oxide pellets have highlighted several challenges and inconsistencies that complicate the understanding of the effects of TiO$_2$. A major problem has been the different experimental conditions in the different studies, including differences in temperature, gas composition, and pellet formulations, which have led to inconsistent results regarding the catalytic role of TiO$_2$. In addition, many studies have focused narrowly on specific aspects of the reduction process, often ignoring wider effects such as slag flowability and pellet mechanical properties. This narrow focus leads to incomplete findings and limits the practical applicability of the results. In addition, there is a notable lack of long-term performance data, especially regarding the stability and durability of TiO$_2$-enriched pellets in continuous industrial operation, which is crucial for their potential scaling up and commercial application. These gaps and inconsistencies highlight the need for a more standardized and comprehensive approach to exploring the role of TiO$_2$ in the reduction of iron oxide

pellets. The study aims to shed light on the mechanisms underlying these effects, which have previously shown variations across different experimental conditions and have been subject to differing interpretations in the literature.

The scientific significance of this study lies in its contribution to advancing our understanding of the fundamental processes involved in the direct reduction of iron oxide pellets. By examining parameters such as reduction rate, diffusion coefficient, and time to reduction, the research seeks to elucidate the specific mechanisms through which TiO_2 influences the reduction behavior of iron ore. Furthermore, by comprehensively exploring these dynamics, the study addresses technical difficulties associated with optimizing reduction processes in industrial settings, offering insights that could inform the development of more efficient and sustainable iron production methods.

II. EXPERIMENTAL PROCEDURE

The pellets analyzed in the present study were provided by VALE (Brazil), where the production process of the pellets is described in detail in Reference 8. The average chemical composition of the pellets which taken from the twenty pellets is shown in Table I. The pellets selected had a good spherical shape with the diameter in the range of 1 to 2 cm (Figure 1), density range between 3600 and 5200 kg/m^3, and specific surface ranging of 1500 to 1600 cm^2/g. The density of the pellets was measured by measuring seven diameters of the pellets. After calculating the average diameter of the pellets, this was used to calculate the density after the pellets were weighed with a precision balance. The pellet reduction experiments were carried out in a self-designed and developed shaft furnace (Figure 2).

The direct reduction experiments were carried out in a temperature range of 900 °C to 1000 °C. The gas composition was 100 pct hydrogen, 50 pct H_2 + 50 pct CO and 100 pct CO. The reduction pressures used were 1-5 bar. The flow of reducing gas was between 1 and 5 L/min and the basicity index (referred as the CaO/SiO_2

Fig. 1—Pellets employed in the present study.

Fig. 2—Self-designed shaft furnace.

ratio) between 0 and 2.15. Basicity has a considerable influence on the quality of iron ore pellets. A higher basicity promotes the formation of calcium ferrite, which improves reducibility, while too high a basicity can led to free lime, which reduces the strength of the pellets. An appropriate degree of basicity improves cold break resistance, which is important for transport and handling, and optimizes reducibility. It minimizes swelling during reduction, prevents the pellets from disintegrating in the blast furnaces, and ensures efficient processing. Table II provides a comparative overview of the experimental conditions used in various studies, including the current research.

The shaft furnace was equipped with a precise temperature control system that allowed a constant temperature range of 900 °C to 1000 °C. The pellets were carefully selected for uniform shape and size and had a diameter of 1 to 2 cm. They were systematically weighed with a precision scale to ensure an accurate measurement of their mass before they were introduced into the furnace. Initially, the oven was preheated to the desired temperature at a controlled heating rate. Once the target temperature was reached, a predetermined

Table I. The Average Composition of Charging Pellets, Wt Pct

Fe_2O_3	CaO	TiO_2	MgO	Al_2O_3	SiO_2
96.63	1.02	0	0	0.38	1.97
82.93	1.63	0.19	4.69	2.93	7.63
88.27	0.68	3.36	0.88	1.89	4.92
95.46	1.80	0.04	0.60	0.50	1.60
97.03	1.00	0.18	0.69	0.20	0.90
96.60	1.00	0.09	0.06	0.53	1.72
97.25	1.62	0.02	0.02	0.33	0.75
97.05	0.73	0.19	0.57	0.40	1.06
96.88	**0**	**0.92**	**0**	**0.70**	**1.50**
98.17	0.06	0.03	0.03	0.44	1.25
87.09	1.29	0.23	2.02	1.68	7.69

The composition of the pellets whose reduction curve is shown in Figure 13 and microstructure in Figure 14 are given in bold.

amount of pellets, usually around 20g, was placed into the oven. The system was then sealed to prevent atmospheric gasses from entering and affecting the reduction process. For the gas flow and composition, the reduction gasses used were either 100 pct hydrogen, a mixture of 50 pct hydrogen, and 50 pct carbon monoxide or 100 pct carbon monoxide, depending on the specific experimental conditions. The flow rate of these gasses was carefully controlled between 1 and 5 L/min using precise flow meters and regulators. Throughout the experiment, the pressure inside the oven was kept between 1 and 5 bar to simulate different industrial conditions. This pressure was continuously monitored and adjusted as necessary to ensure it remained within the specified range. At the end of each reduction experiment, the gas supply was turned off and the system was purged with nitrogen to safely remove residual reactive gasses and gradually cool the pellets to room temperature. This method of cooling was crucial to maintain the reduced state of the pellets and prevent reoxidation. Three tests were carried out for each condition to ensure the reproducibility of the result.

The pellets pores aspect and evolution were analyzed by microtomography by employing a Phoenix v/tome/x s (General Electric). X-ray computed microtomography is a nondestructive technique that allows the internal and three-dimensional visualization of a sample subjected to a source of ionizing radiation with virtually no need for physical and chemical preparations of the pellet. It is based on the same principles as conventional radiography, where each part of a sample absorbs the rays differently. In this way, it is possible to study the two-dimensional cross sections in a nondestructive way and through mathematical principles, it is possible to reconstruct them in order to build the respective three-dimensional model of the sample, allowing thus the visualization and quantification of the internal structure of the material. Computed tomography produces an image very close to the reality by displaying the average attenuation of each small volume element, ordering the beam attenuation information and translating the information quantitatively.[9,34,35] Pore segmentation was performed with the help of free software FIJI/ImageJ. A lower limit was visually determined where some pores were not selected, and an upper limit, where pores that have not been previously filled can be selected. The threshold (maximum or minimum) can be fixed for all sample layers. Determining the threshold is important because it has a great impact on obtaining the porosity percentage of iron ore pellets.[9] The reduction curves (percentage of reduction versus time to reduction) were used to calculate the kinetic constants and reduction rates as described in the next section. The etails of the experiment have been described in previ us publications of our group.[9,36,37] It is worth noting at the decision to choose relatively small intervals for as proportion and temperature was aimed at capturing etailed variations and trends in the reduction param ers. Although smaller intervals allow a more detailed vestigation of the parameter space, they can also lead difficulties in determining the exact optimum. There re, caution is advised in interpreting the results within

the chosen intervals and that future research examining a wider parameter space may provide additional insight and validation of our results.

The experimental design included a systematic investigation of the processing parameters and variations in pellet composition to understand their combined effect on the efficiency of the direct regeneration processes. For this purpose, the data from the reduction experiments were modeled with respect to the processing parameters and the properties of the pellets and the results were analyzed using the multi-objective software modeFrontier. Further details on the method used can be found in References 9, 38, and 39. The optimization algorithms of the Pareto frontier were used to determine the best possible solutions, which become the optimal solutions. The analyses performed by modeFrontier go beyond the gradient methods, in which the algorithms search for either the minimum or the maximum of an objective function, depending on the objective. The first important result is therefore the appropriate weighted effect of each individual input parameter considered on a particular output. In this way, it is possible to determine which parameters influence the analyzed process most effectively. This also makes it possible to separate the objectives in the case of the optimization step. In the case of very complex analyses (inputs and outputs), the optimization naturally leads to a profound compromise between many potential optimal solutions. Thus, the final optimization algorithm will present many results that lie on the Pareto frontier for trade-offs. These solutions all have the property that none of the objectives can be improved without compromising another one.[39] In our experience to date, the software has been used very successfully to analyze processes in iron and steel production.[37,40]

Physical and mathematical functions are introduced here that represent the reduction process. The data flow contains all input parameters namely reduction temperature, reduction pressure, basicity index, pellet density, total Fe (TFe), TiO_2 content, kinetic constant (k), reduction rates (from equations (1) and (2)), time to 95 pct reduction, that were optimized in the numerical simulations. These were used to define the so-called scatter matrix, in which the weight of each input on the variation of a given output is immediately defined numerically between - 1 and + 1. If the correlation factor is – 1, this means that the input and output are perfectly inversely proportional. On the other hand, if the correlation factor is + 1, the input and output are directly proportional.

III. RESULTS

In order to investigate the effects of the amount of TiO_2 on the reduction behavior of the iron oxide, various parameters were evaluated in different reduction atmospheres and at different temperatures. The reduction rate $\left(\frac{\mathrm{d}R}{\mathrm{d}t}\right)$ was determined by dividing the experimental mass loss by the theoretical mass loss, whereby the hematite in the pellet was considered to be

Table II. Comparative Summary of the Experimental Conditions in Various Studies on the Reduction of Iron Oxide Pellets

Study Reference	TiO$_2$ content (wt pct)	Temperature Range (°C)	Reducing Gas Composition	Pressure Range (bar)	Basicity Index Range
Current Study	0 to 3.36	900 to 1000	100 pct H$_2$, 50 pct H$_2$ + 50 pct CO, 100 pct CO	1 to 5	0 to 2.15
Paananen et al.[11]		850 to 950	80 pct H$_2$ + 20 pct CO	1 to 3	0.5 to 1.5
Pimenta et al.[21]	0.07 to 0.7	800 to 1100	70 pct H$_2$ + 30 pct CO	2 to 6	0.3 to 2.0
Ju et al.[7]	5	600 to 1220	20 pct H$_2$ + 80 pct CO	1.5 to 3.5	0.8 to 1.8
Tang et al.[12]	4.48	1000 to 1100	28 pct H$_2$ + 72 pct CO; 50 H$_2$ + 50 CO;	1	0.1
Yu et al.[23]	20	500 to 1050	100 pct H$_2$	1	0.46
Scharm et al.[33]	0.73 to 0.86	800 to 1100	100 pct H$_2$ and 100 pct CO	1	0.7 to 0.74

completely reduced to iron. The reduction rate (quantified as mass loss per time) was also analyzed using the following two indexes[36]:

$$\frac{dR}{dt_{40}} = \frac{33.6}{t_{60} - t_{30}} \qquad [1]$$

$$\frac{dR}{dt_{90}} = \frac{13.9}{t_{95} - t_{80}} \qquad [2]$$

with t_{95}, t_{90}, t_{80}, t_{60}, and t_{30} being the time required to reduce the pellets by 95, 90, 80, 60, and 30 pct.

Figure 3 illustrates variations in the dR/dt40 with varying TiO$_2$ amounts and basicity index across different reducing atmospheres and temperatures. One crucial consideration is the notable influence of TiO$_2$ amount as a parameter affecting the reduction rate. This impact undergoes noticeable changes in diverse reducing conditions. In the 100 pct CO reducing atmosphere at 1000 °C, as depicted in Figure 3(a), an increase in the TiO$_2$ amount up to 1.5 pct results in a decrease in the reduction rate, irrespective of the basicity index. However, for TiO$_2$ amounts exceeding approximately 1.5 pct, a contrary trend emerges, with the reduction rate increasing alongside higher TiO$_2$ amounts. Therefore, the range of 1 to 1.5 pct TiO$_2$ can be identified as a transitional region for the TiO$_2$ effect on the reduction rate of iron oxide. In fact, the dR/dt40 is highest with lower TiO$_2$ amounts and medium basicity index. Figure 3(b) reveals similar variations in the 50 pct CO-50 pct H$_2$ atmosphere, where an increase in TiO$_2$ amount initially leads to a reduction in the rate, up to about 2 pct of TiO$_2$, regardless of the basicity index. However, further enhancement in TiO$_2$ results in an increased reduction rate. The presence of 50 pct H$_2$ in the reducing gas expands the transition region from 1 to 1.5 to 1.5 to 2 pct. Moreover, Figure 3(b) demonstrates that the presence of H$_2$ significantly boosts the reduction rate, scaling up almost four times compared to the 100 pct CO atmosphere. It is worth mentioning that in the presence of 50 pct H$_2$ gas, the influence of the basicity index on the reduction rate becomes noticeable.

As a matter of fact, the addition of H$_2$ to the atmosphere changes the reduction behavior significantly, resulting in a very high reduction rate across almost all basicity indexes with lower TiO$_2$ amounts. This suggests that H$_2$ is very effective at reducing iron ore at high temperatures, even more so than CO in certain conditions, possibly because H$_2$ can penetrate the ore more readily and react with iron oxide at lower temperatures. In addition, the reduction rate increases with the rise in the basicity index, thereby mitigating the impact of the TiO$_2$ amount.

Variations in the reduction rate under a 100 pct H$_2$ reducing atmosphere at both 1000 and 900 °C are illustrated in Figures 3(c) and (d), respectively. It is notable that the impact of different parameters on the reduction process in the H$_2$ atmosphere differs from that in the CO atmosphere. In fact, under a full H$_2$ atmosphere at 1000 °C, the reduction rate is again high across the board but starts to decrease more significantly with higher TiO$_2$ content. Figure 3(c) demonstrates that, at 1000 °C, there is an increase in the reduction rate with the addition of TiO$_2$ up to 0.5 pct. However, beyond this transition point, a further increase in TiO$_2$ leads to a decrease in the reduction rate, showcasing an inverse behavior compared to the reduction process in the presence of CO gas. Additionally, it is worth emphasizing that the magnitude of the reduction rate in the presence of H$_2$ gas, regardless of the temperature, is twice as high as the reduction rate in the presence of 50 pct CO-50 pct H$_2$ and almost 20 times higher than the reduction rate in the presence of 100 pct CO gas. This significant difference underscores the distinct influence of H$_2$ as a reducing agent, highlighting its potential for enhancing the reduction kinetics. At a lower temperature of 900 °C, the effectiveness of H$_2$ in reducing the ore is lessened, which is evident from the overall lower reduction rates compared to the 1000 °C condition. However, the plot still shows that a lower TiO$_2$ content and a basicity index around 0.5 to 1.5 is where the reduction rate is higher, suggesting that these are the more optimal conditions at this temperature. Moreover, this observation suggests that the role of TiO$_2$ in influencing the
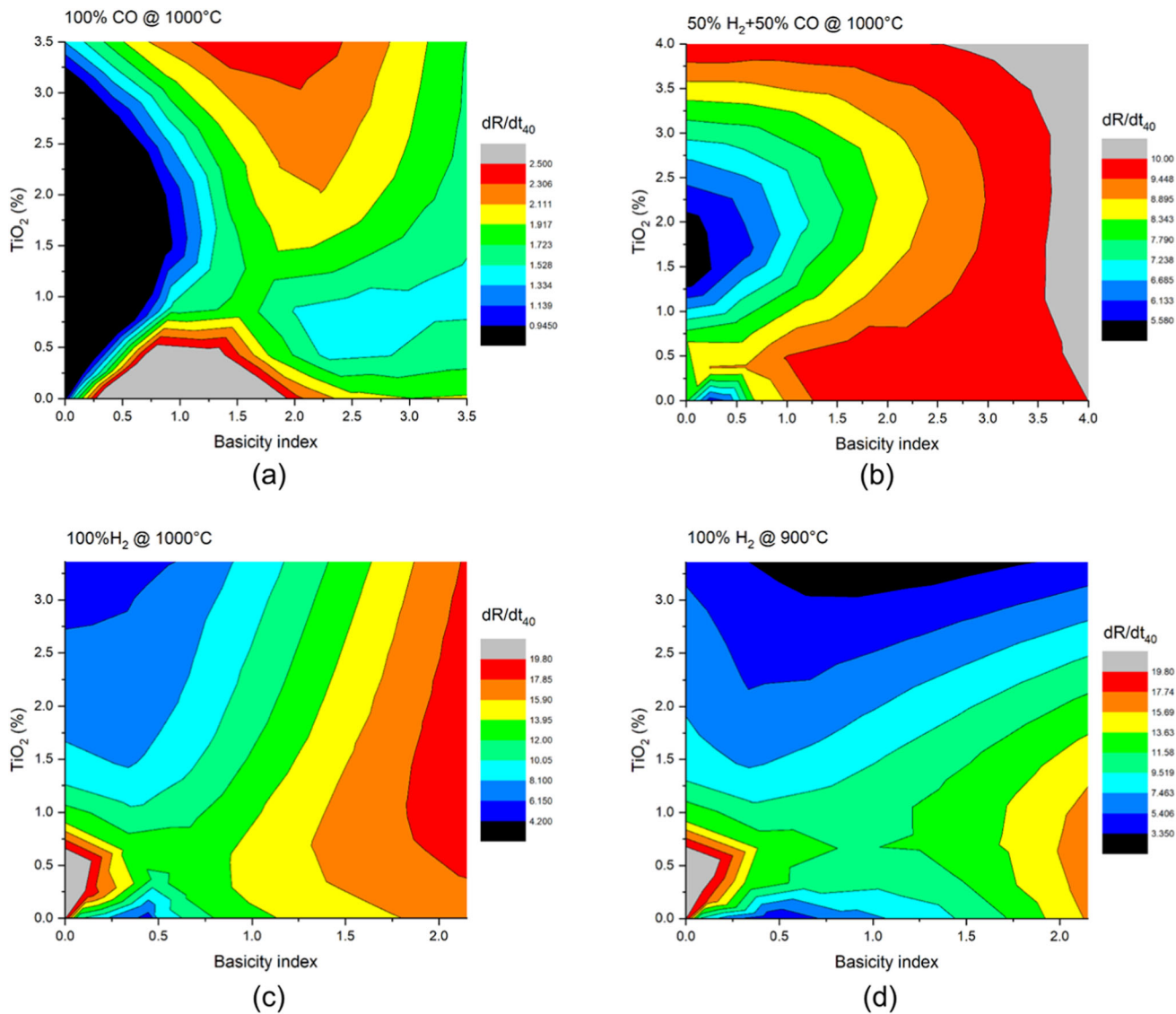
Fig. 3—The 2D maps revealing the variations in reduction rate (dR/dt40) as a function of the TiO_2 amount and the basicity index of the Iron ore in the (*a*) 100 pct CO atmosphere at 1000 °C, (*b*) 50 pct CO-50 pct H_2 atmosphere at 1000 °C, (*c*) 100 pct H_2 atmosphere at 1000 °C, and (*d*) 100 pct H_2 atmosphere at 900 °C.

reduction rate is more delicate in the H_2 atmosphere compared to the CO atmosphere, necessitating a careful examination of the interplay between these variables for a comprehensive understanding of the reduction process. However, it can be concluded that 0.5 pct of TiO_2 seems an optimum point for TiO_2 amount in the reduction process of the Iron oxide in the presence of 100 pct H_2.

The reduction rate was further investigated using the dR/dt90 parameter, and the 2D maps illustrating the impact of TiO_2 amounts on this parameter under various reducing conditions are presented in Figure 4. Figure 4(a) demonstrates that the dR/dt90 in a 100 pct CO atmosphere at 1000 °C exhibits a behavior similar to that of the dR/dt40 parameter. An increase in the TiO_2 amount initially results in a reduction in the rate, and after a transition region, identified here as 2-2.5 pct TiO_2, the behavior shifts, leading to an increase in the

reduction rate with higher TiO_2 amounts. The introduction of 50 pct H_2 to the reduction atmosphere induces changes in the reduction behavior, as illustrated in Figure 4(b). It is evident that the reduction rate is significantly influenced by TiO_2, especially for amounts exceeding 1.5 pct, where the rate increases with the TiO_2 amount. However, beyond a basicity index of 3, this relationship undergoes a shift, and the reduction rate becomes less affected by the TiO_2 amount. Additionally, it is observed that the reduction rate is more intensively influenced by the basicity index, particularly for TiO_2 amounts below 2 pct. Notably, a higher reduction rate is evident in the presence of 50 pct H_2 compared to the 100 pct CO atmosphere.

The 2D maps depicted in Figures 4(c) and (d) showcase the reduction behavior of iron oxide concerning TiO_2 amounts and basicity in the presence of a 100 pct H_2 atmosphere at 1000 and 900 °C, respectively.
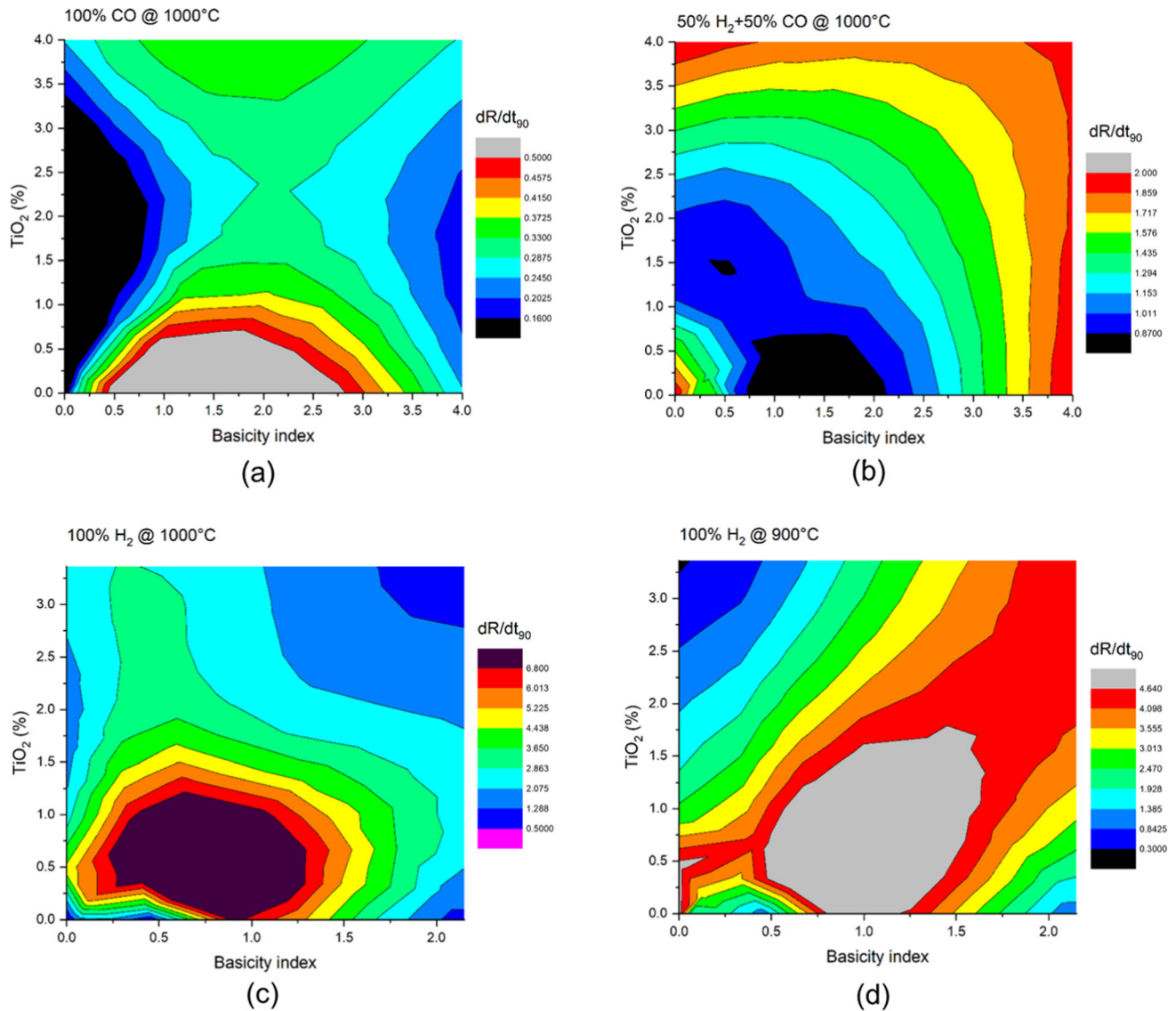
Fig. 4—The 2D maps revealing the variations in reduction rate ($dR/dt90$) as a function of the TiO_2 amount and the basicity index of the Iron ore in the (*a*) 100 pct CO atmosphere at 1000 °C, (*b*) 50 pct CO-50 pct H_2 atmosphere at 1000 °C, (*c*) 100 pct H_2 atmosphere at 1000 °C, and (*d*) 100 pct H_2 atmosphere at 900 °C.

In the context of 100 pct H_2, it is evident that for TiO_2 amounts below 0.5 pct, the reduction rate decreases with a reduction in TiO_2 amount. Conversely, for higher TiO_2 amounts, the reduction rate decreases with an increase in TiO_2 amount, highlighting 0.5 pct TiO_2 as an optimal point for iron oxide reduction in the presence of a 100 pct H_2 reducing gas (refer to Figure 4(c)). Additionally, Figure 4(c) illustrates that with an increase in the basicity index, the reduction rate decreases, which contrasts with the behavior observed in the $dR/dt40$ parameter. It is noteworthy that the scale of the $dR/dt90$ parameter in the presence of 100 pct H_2 is higher than that of the 100 pct CO, indicating an increase of ten times. Reducing the process temperature to 900 °C in the presence of H_2 as the reducing gas does not alter the observed behavior, and an optimum amount of 0.5 pct TiO_2 is evident. In this scenario, the reduction rate reaches its maximum and subsequently decreases with

both an increase and decrease in the TiO_2 amount. This consistent behavior across temperatures further underscores the significance of the 0.5 pct TiO_2 threshold for achieving optimal iron oxide reduction in the presence of a 100 pct H_2 atmosphere.

The variations in reduction time were examined as a function of the TiO_2 amount under different conditions, and the results are presented in Figure 5. The initial consideration pertains to the time scale for reduction in various atmospheres. The maximum time is observed in the 100 pct CO atmosphere, and as the H_2 amount increases, the time scale noticeably decreases, reaching its minimum in the 100 pct H_2 atmosphere at 1000 °C. However, a slight increase is noted with a temperature reduction to 900 °C. In Figure 5(a), it is evident that in the 100 pct CO atmosphere, the reduction time is not strongly dependent on the TiO_2 amount up to 1.5 pct TiO_2, particularly in the range of basicity index from 0.5
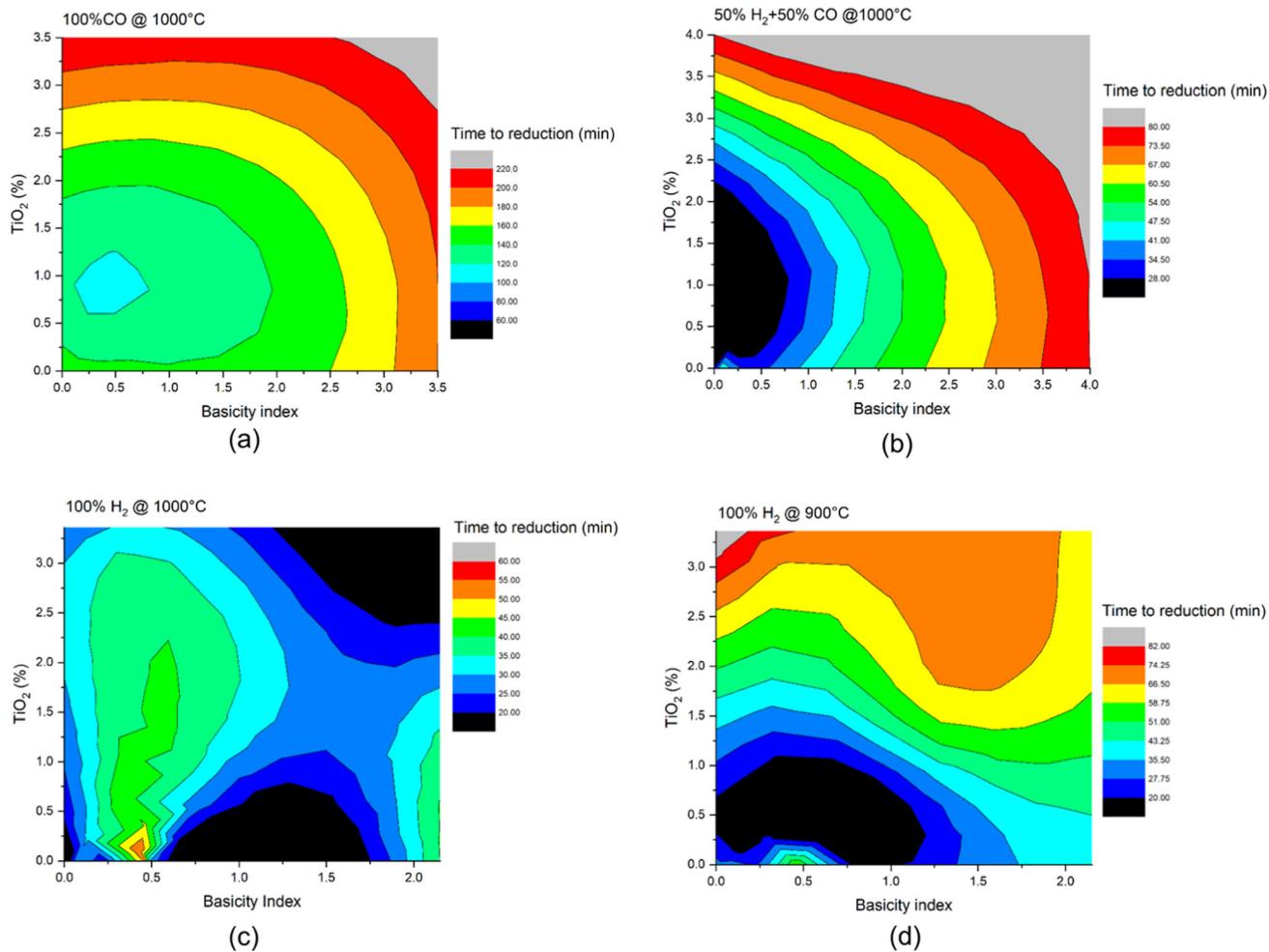
Fig. 5—Variations in time to reduction as a function of the TiO_2 amount and the basicity index of the Iron ore in the (*a*) 100 pct CO atmosphere at 1000 °C, (*b*) 50 pct CO-50 pct H_2 atmosphere at 1000 °C, (*c*) 100 pct H_2 atmosphere at 1000 °C, and (*d*) 100 pct H_2 atmosphere at 900 °C.

to about 2.5; however, at a high basicity index (above 2.5 pct) , the reduction time increases with an increase in the TiO_2 amount (above 1.5 pct). Additionally, the figure illustrates that at lower TiO_2 levels, the time to reduction is strongly affected by the basicity index, increasing with a rise in the basicity index. Introducing 50 pct H_2 to the reducing atmosphere results in a reduction of the time scale by almost three times compared to the 100 pct CO atmosphere, as shown in Figure 5(b). Furthermore, it becomes apparent that the minimum time to reduction is associated with the minimum TiO_2 amount and basicity index. With an increase in these parameters, the reduction time also increases. Notably, the dependency of the reduction time on the basicity index intensifies in the presence of 0 pct H_2. - There is a noticeable minimum time to reduction at a basicity index of around 1.5, suggesting n optimal basicity level for the reduction in this mixed tmosphere. This underscores the intricate relationship etween TiO_2 amounts, basicity index, and the nature of e reducing atmosphere in determining the reduction me for iron oxide. Figure 5(c) depicts variations in duction time in the 100 pct H_2 atmosphere at 1000 °C.

The map shows a trend of increasing time to reduction with higher TiO_2 content, but overall, the times are much lower than those in the CO or CO-H_2 atmospheres. Notably, compared to other conditions, the time to reduction decreases significantly, highlighting the efficacy of the H_2 atmosphere for iron oxide reduction. However, this figure also reveals that the reduction time is not directly dependent on the TiO_2 amount, exhibiting oscillations with changes in TiO_2 levels. Despite this, a comprehensive examination of the 2D map suggests that, on the whole, an increase in the basicity index correlates with a decrease in reduction time. As demonstrated in Figure 5(d), a decrease in the temperature results in an increase in the time to reduction. The higher time to reduction at this lower temperature indicates that temperature is a critical factor in H_2-based reduction, with higher temperatures leading to faster reactions. Therefore, from kinetic point of view, it can be inferred that in the 100 pct H_2 atmosphere, the presence of TiO_2 is not conducive to reduction, as an increase in the TiO_2 amount corresponds to an increase in reduction time.

The kinetic parameter (k diffusion) was investigated as a function of TiO_2 amount, basicity index, and the reduction atmosphere, as illustrated in 2D maps in Figure 6. Calculated through the three-dimensional diffusion model and phase boundary controlled reaction[36,41]:

$$k = \frac{[1 - (1 - \alpha)^{\frac{1}{3}}]^2}{t} \qquad [3]$$

$$k = \frac{1 - (1 - \alpha)^{\frac{1}{3}}}{t} \qquad [4]$$

where α represents the fraction reacted (0–1) and t is the time at which a given fraction of the material reacts. In Figure 6(a), it is evident that the k parameter is strongly influenced by the TiO_2 amount, increasing as the TiO_2 amount in the iron ore rises. This

trend is more pronounced at a higher basicity index. Additionally, the k diffusion is dependent on basicity, with the parameter decreasing with an increase in the basicity index up to 2 pct, then reversing and increasing again. The introduction of 50 pct H_2 to the reducing gas, as shown in Figure 6(b), leads to an overall increase in the k diffusion parameter, particularly at lower TiO_2 contents and a basicity index range of approximately 0.5 to 2.5. However, a distinct behavior is observed where the maximum k parameter is reached at both the maximum TiO_2 amount with the minimum basicity index and the maximum basicity index with the minimum TiO_2 amount. In Figure 6(c), it is revealed that reduction in a 100 pct H_2 atmosphere results in the maximum k diffusion, three times more than the sample reduced in the 100 pct CO atmosphere. Additionally, the highest k diffusion values occur at lower TiO_2 contents and lower basicity indexes. Decreasing the temperature to 900 °C, as
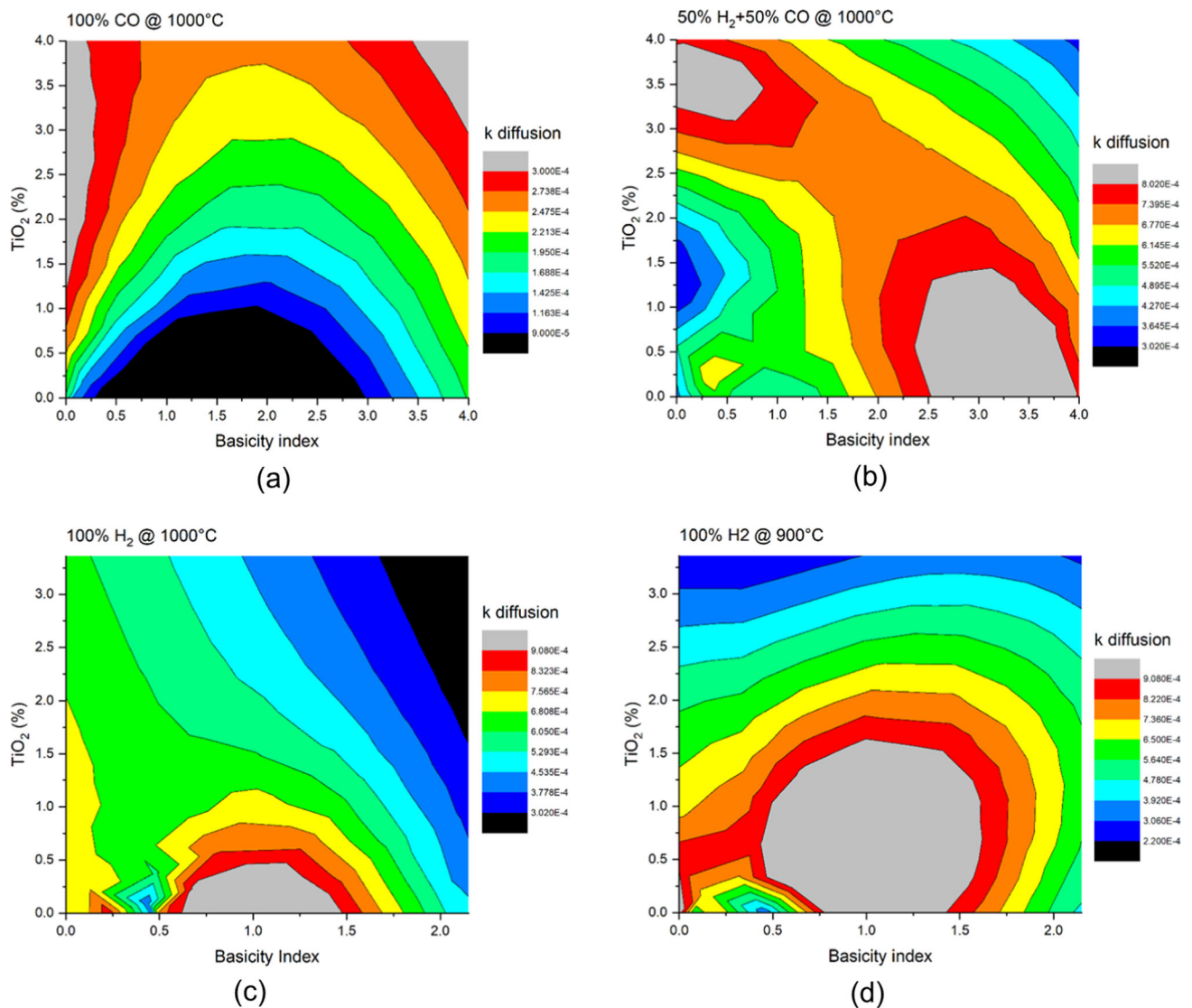

Fig. 6—The 2D maps of the variations in k diffusion with the TiO_2 amount and the basicity index in the (a) 100 pct CO atmosphere at 1000 °C, (b) 50 pct CO-50 pct H_2 atmosphere at 1000 °C, (c) 100 pct H_2 atmosphere at 1000 °C, and (d) 100 pct H_2 atmosphere at 900 °C.

METALLURGICAL AND MATERIALS TRANSACTIONS B

depicted in Figure 6(d), does not strongly impact the k parameter; however, it seems that this parameter becomes more sensitive to the TiO_2 amount and basicity index. Despite the lower temperature, the map shows that a lower TiO_2 content and a basicity index between approximately 0.5 and 1.5 have higher k diffusion values, suggesting that these conditions are still favorable for H_2 diffusion, albeit to a lesser extent than at the higher temperature.

The 2D maps presented in Figure 7 reveal the effects of varying amounts of TiO_2 and pressure on different parameters of the iron reduction process in a 100 pct H_2 atmosphere at 1000 °C. As shown in Figure 7(a), as the pressure increases, the reduction rate generally increases. This is likely due to the increased partial pressure of H_2, which drives the reduction reaction forward more effectively. The influence of TiO_2 on the reduction rate is less clear, but there seems to be a moderate range of TiO_2 amounts where the reduction rate is optimal, neither at the lowest nor at the highest TiO_2 content. This could be due to the complex role of TiO_2 in the reduction process, where it can act as a catalyst at certain concentrations, but can also form stable compounds that are more difficult to reduce. Furthermore, Figure 7(b) illustrates that at low TiO_2 amounts, the reduction time is unaffected by pressure. However, for TiO_2 amounts exceeding 0.5 pct, the pressure has a noticeable effect, reducing the time to reduction with an increase in pressure, indicating a positive influence of pressure on the reduction process. In fact, increasing TiO_2 content appears to increase the time to reduction, suggesting that TiO_2 may have a negative impact on the efficiency of the reduction process.

On the other hand, Figure 7(c) depicts that at low TiO_2 amounts (less than 1.5 pct), pressure does not significantly impact the k diffusion parameter. However, at higher TiO_2 levels, pressure positively affects the process, leading to an increase in k diffusion with a rise in pressure. The diffusion coefficient decreases with increasing pressure. This might seem nonlogical, but at higher pressures, the reduction reaction could be occurring more at the surface of the pellet, reducing the need for H_2 to diffuse throughout the pellet.
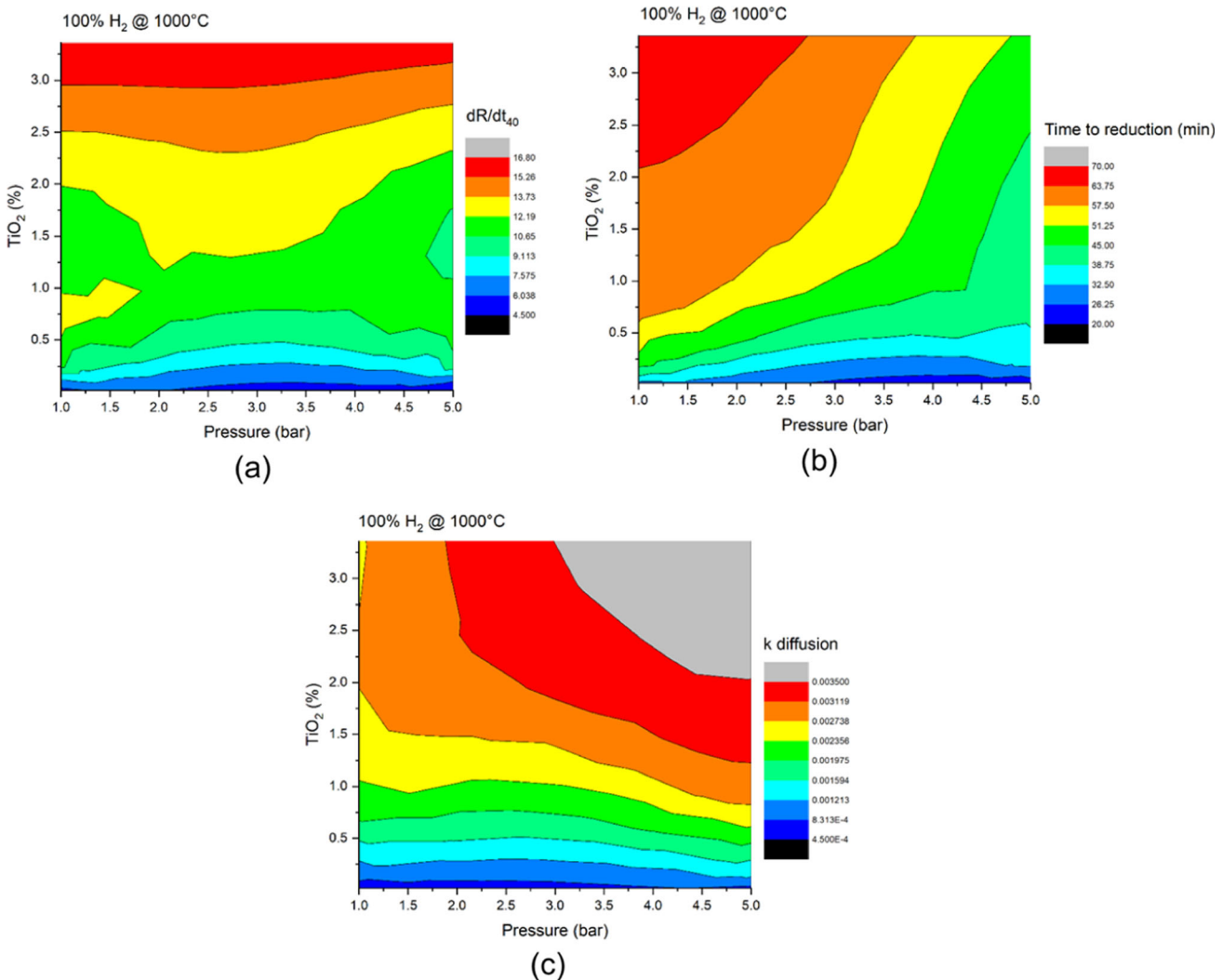
g. 7—2D maps indicating the effects of TiO_2 amount and pressure on the (*a*) dR/dt40, (*b*) time to reduction, and (*c*) k diffusion.
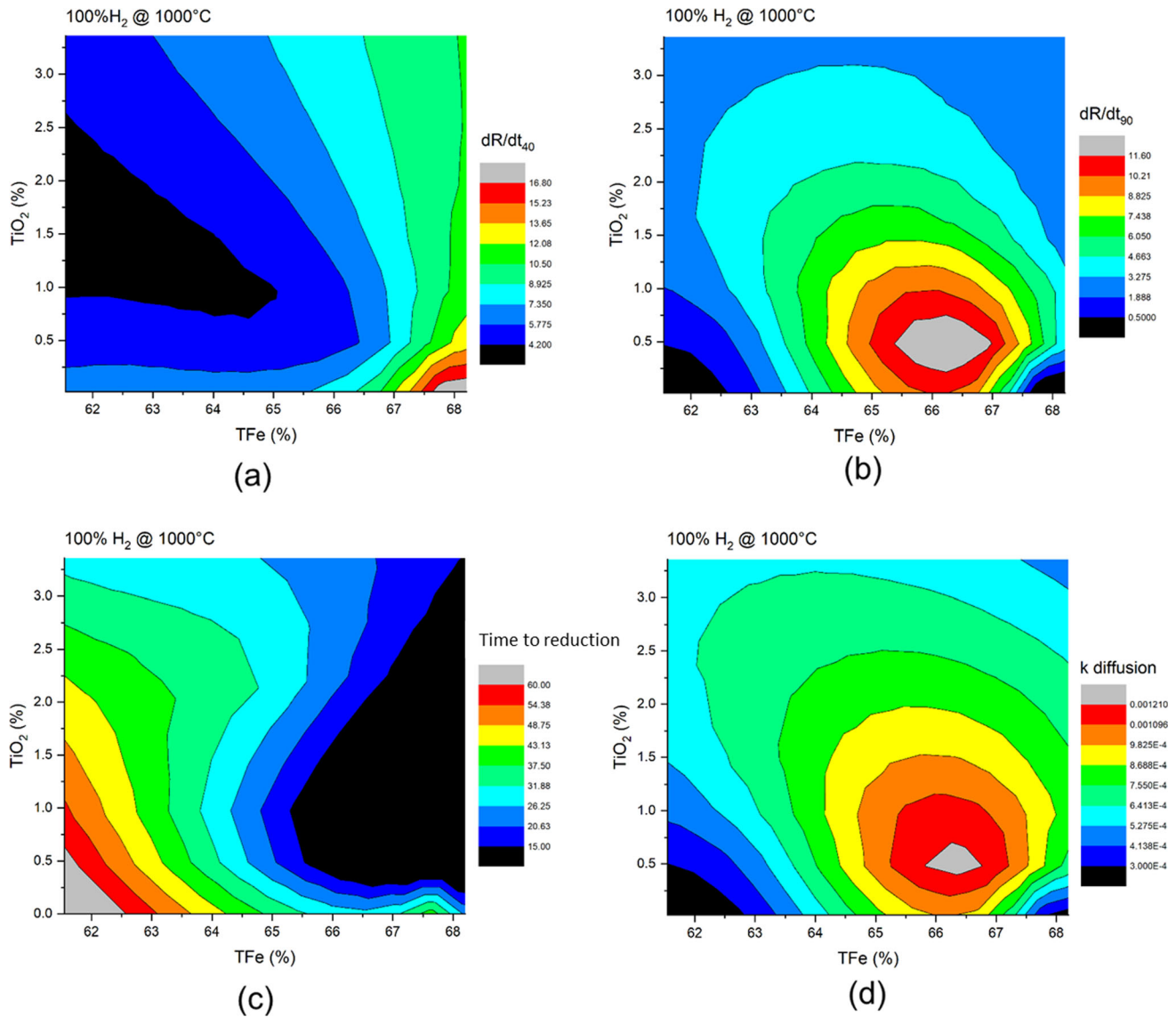
Fig. 8—Effects of *TiO2* amount and TFe on the (*a*) dR/dt40, (*b*) dR/dt90, (*c*) time to reduction, and (*d*) k diffusion.

Figure 8, presenting the variations in 2D maps, depicts the effects of varying TiO_2 content and TFe percentage on different aspects of the iron oxide pellets reduction process in a 100 pct H_2 atmosphere at 1000 °C. A preliminary overview of the findings indicates that TFe is advantageous for the reduction process, likely due to a higher concentration of reducible material. A higher TiO_2 content appears to decrease the reduction rate. As depicted in Figure 8(a), the maximum reduction rate (dR/dt40) occurs at the maximum TFe, gradually decreasing with a decline in TFe. Additionally, variations in the dR/dt90 parameter illustrate an increase with rising TFe, reaching its peak between 65 and 67 pct TFe before decreasing again (refer to Figure 8(b)). This could indicate an optimal range for TiO_2 content where it might facilitate the reduction process. It is noteworthy that dR/dt90 reached its maximum at 0.5 pct TiO_2, and then, decreased with an increase in TiO_2 amount. Figure 8(c) demonstrates the

influence of TFe on the time to reduction, highlighting a strong dependence where reduction time decreases with an increase in TFe. In fact, there is a noticeable increase in reduction times for ore with lower total iron content, particularly below about 64 pct TFe. Moreover, Figure 8(d) indicates the positive effects of TFe on the k diffusion parameter. An increase in TFe enhances k diffusion, reaching its maximum between 65 and 67 pct TFe, followed by a slight decrease with further increases in TFe. The diffusion coefficient is highest at intermediate levels of TiO_2 and TFe content, indicating that a balanced composition facilitates the diffusion of H_2 within the pellet. Therefore, the exploration of reduction parameters in relation to TFe underscores its favorable impact on the reduction process, particularly in enhancing reduction rates, reducing the time to reduction, and positively influencing the k diffusion parameter. These findings contribute valuable insights for optimizing iron oxide reduction processes.

To investigate the effects of TiO$_2$ amount and other parameters on the reduction behavior, the database was analyzed using multi-objective optimization software, namely modeFrontier. The results for different reduction conditions are presented in Figures 9 through 12. Figure 9 illustrates the scatter matrix of iron oxide direct reduction in a 100 pct CO reducing atmosphere at 1000 °C. It is evident that the basicity index, TiO$_2$ amount, and density have almost the same influence on the reduction process, exhibiting a negative effect. This negative effect is characterized by a positive correlation with the reduction time and negative correlations with reduction rates and k diffusion. TFe does not appear to be an influential parameter in this condition. However, gas pressure exhibits a positive influence on the process, showing a negative correlation with reduction time and a positive correlation with reduction rate and k diffusion. Therefore, basicity and TiO$_2$ amount emerge as the two most influential parameters, both demonstrating a negative impact. An increase in either of these parameters can lead to a negative effect on the reduction process.

Figure 10 presents the scatter matrix from the same database in the presence of 50 pct H$_2$ as the reducing gas at 1000 °C. One initial observation is that the influence of all parameters has become mild compared to the process in the presence of 100 pct CO. Basicity index and TiO$_2$ amount remain the two most influential parameters, both exerting a negative influence. Density appears to be ineffective in this condition, and the effect of gas pressure is mild, though it demonstrates a positive impact. The influence of TFe has also undergone slight changes in the presence of 50 pct H$_2$, showing a negative correlation with reduction time and a positive correlation with k diffusion. Therefore, it can be concluded that
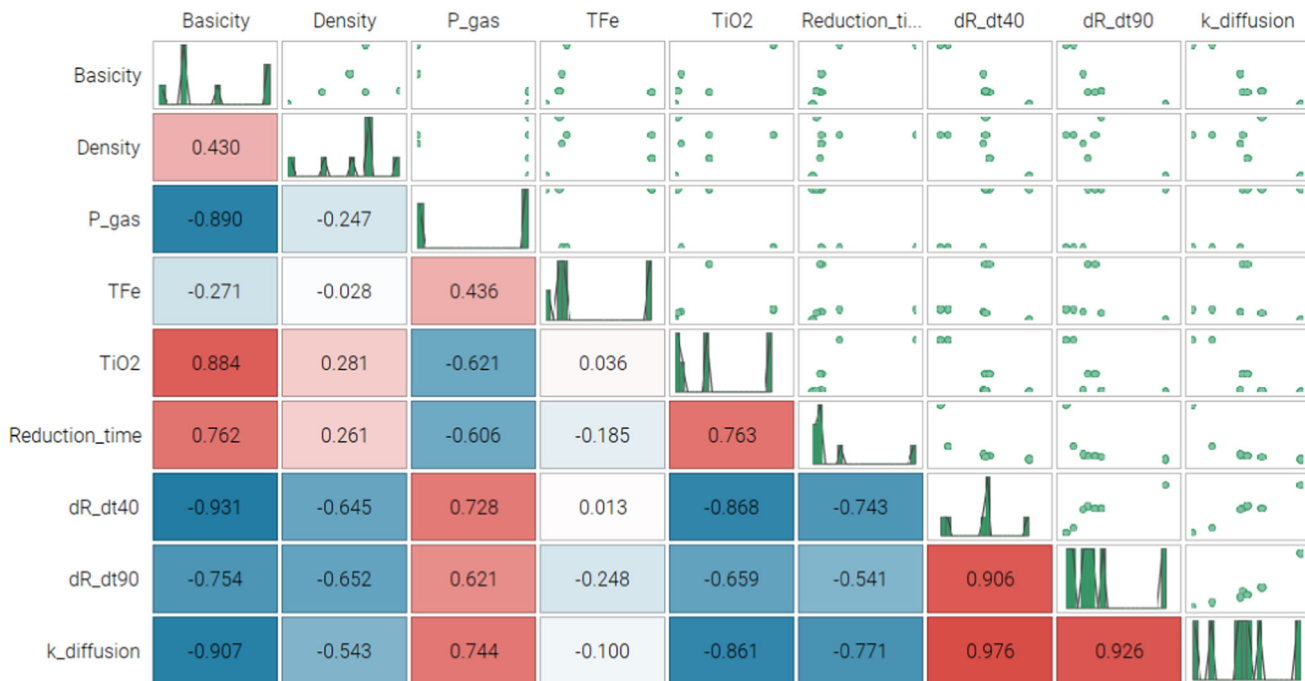
the introduction of 50 pct H$_2$ to the reducing gas diminishes the effectiveness of parameters on the reduction process. However, TiO$_2$ amount remains an influential parameter with a negative impact, suggesting that an increase in this parameter is not favorable for the reduction process.

The scatter matrix of the data processed in the presence of 100 pct H$_2$ as the reducing gas at 1000 °C is presented in Figure 11. It is evident that the effect of the basicity index and TiO$_2$ amount has diminished once again; however, TiO$_2$ can still be considered an effective parameter with a negative influence on the reduction process. The density shows a mild negative effect on the process. Notably, the effect of TFe has become more significant, revealing a strong positive influence on the process. TFe exhibits a negative correlation with the reduction time and a positive correlation with the reduction rate and k diffusion.

Figure 12 illustrates the scatter matrix of iron oxide direct reduction in a 100 pct H$_2$ reducing atmosphere at 900 °C. It is apparent that a decrease in temperature has altered the effectiveness of the parameters, with a noticeable reduction in their influence. However, gas pressure and the TiO$_2$ amount still exhibit a predominantly negative effect, especially on dR/dt90 and k diffusion, indicating negative correlations.

IV. DISCUSSION

To simplify the analysis and interpretation of the results and the data extract from the scattering matrices, different non-ferrous oxides together with different processing parameters were defined as input data and the activity of the iron compounds as output, in

g. 9—Scatter matrix of the Iron oxide direct reduction of the pellets in the presence of 100 pct CO as the reducing gas at 1000 °C.
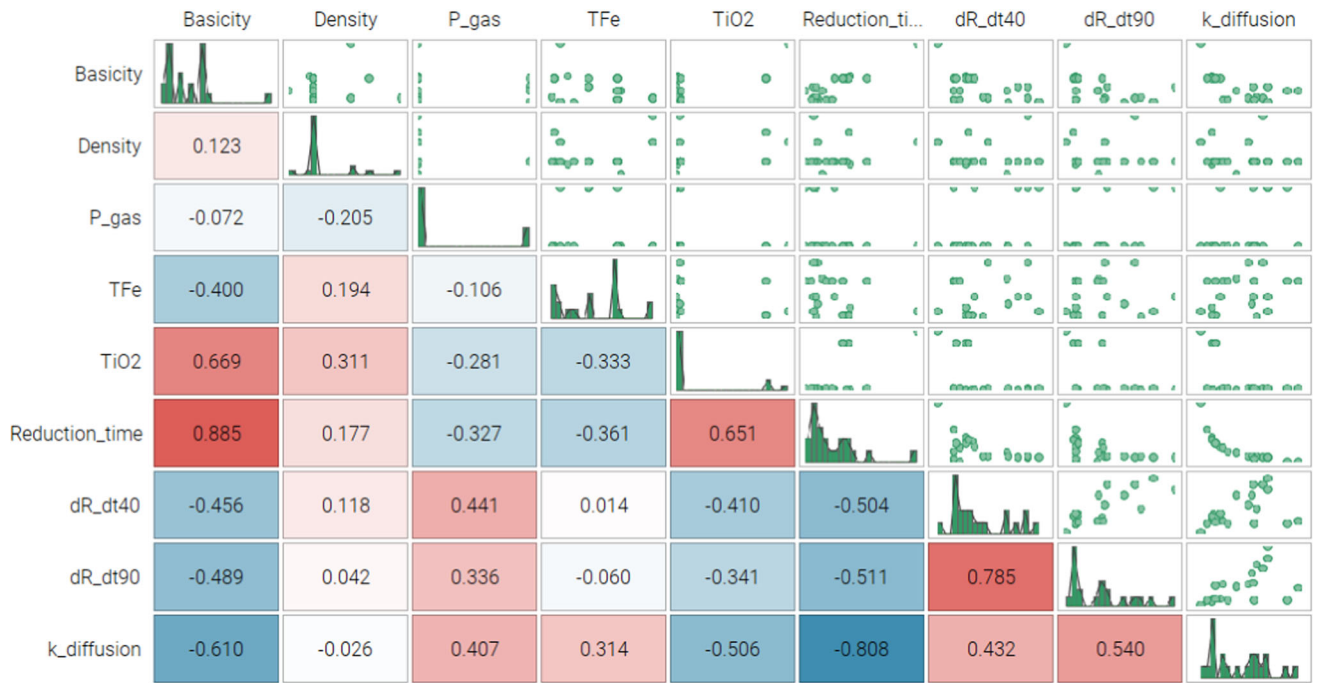
Fig. 10—Scatter matrix of the Iron oxide direct reduction of the pellets in the presence of 50 pct H_2 and 50 pct CO as the reducing gas at 1000 C.
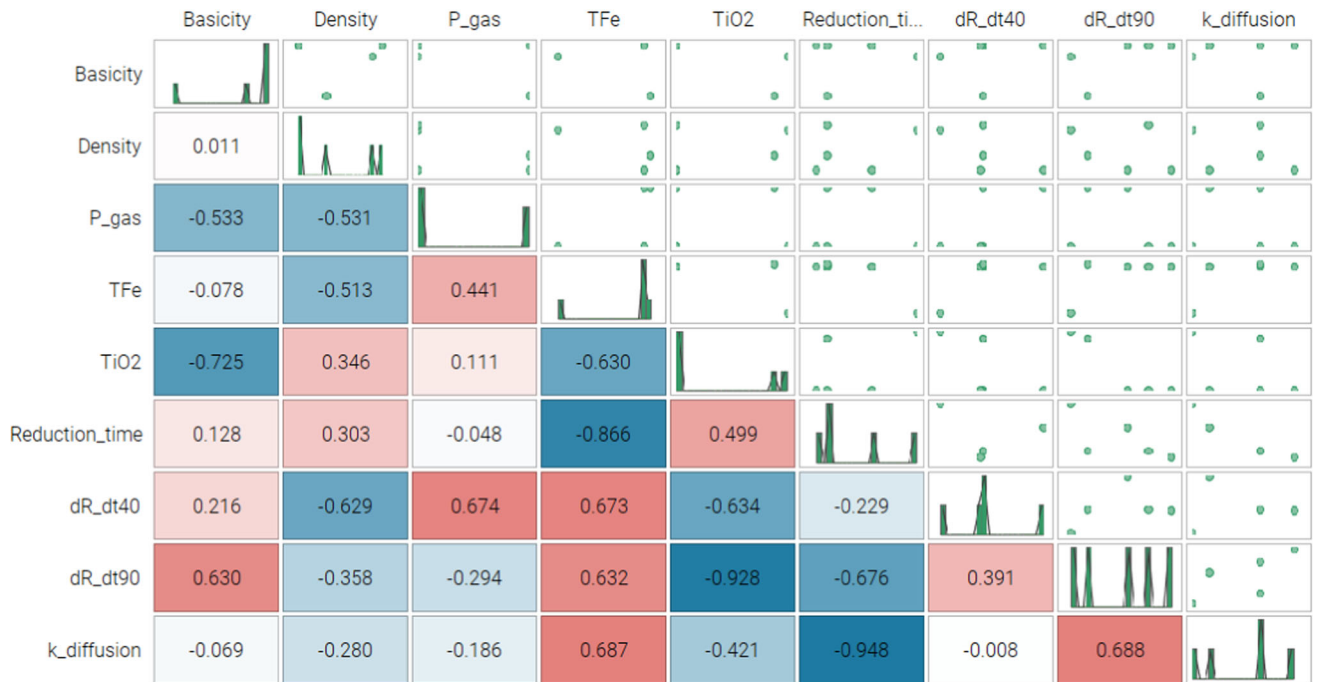
	Basicity	Density	P_gas	TFe	TiO2	Reduction_ti...	dR_dt40	dR_dt90	k_diffusion
Basicity									
Density	0.123								
P_gas	-0.072	-0.205							
TFe	-0.400	0.194	-0.106						
TiO2	0.669	0.311	-0.281	-0.333					
Reduction_time	0.885	0.177	-0.327	-0.361	0.651				
dR_dt40	-0.456	0.118	0.441	0.014	-0.410	-0.504			
dR_dt90	-0.489	0.042	0.336	-0.060	-0.341	-0.511	0.785		
k_diffusion	-0.610	-0.026	0.407	0.314	-0.506	-0.808	0.432	0.540	

Fig. 11—Scatter matrix of the Iron oxide direct reduction of the VALE pellets in the presence of 100 pct H_2 as the reducing gas at 1000 C.

	Basicity	Density	P_gas	TFe	TiO2	Reduction_ti...	dR_dt40	dR_dt90	k_diffusion
Basicity									
Density	0.011								
P_gas	-0.533	-0.531							
TFe	-0.078	-0.513	0.441						
TiO2	-0.725	0.346	0.111	-0.630					
Reduction_time	0.128	0.303	-0.048	-0.866	0.499				
dR_dt40	0.216	-0.629	0.674	0.673	-0.634	-0.229			
dR_dt90	0.630	-0.358	-0.294	0.632	-0.928	-0.676	0.391		
k_diffusion	-0.069	-0.280	-0.186	0.687	-0.421	-0.948	-0.008	0.688	

accordance with the objective of this work. The scatter plots are located at the top right of the matrix and the univariate histograms on the diagonal. The lower left part shows the correlation coefficients. The green circles show how well the design space is fulfilled and how the inputs influence the outputs. A numerical index of $+1$ indicates a direct effect, while -1 indicates an inverse relationship.

The results demonstrated the reduction behavior of iron oxide pellets under different conditions has revealed a dynamic relationship between the TiO_2 content and the reducibility of these pellets. Our results show that
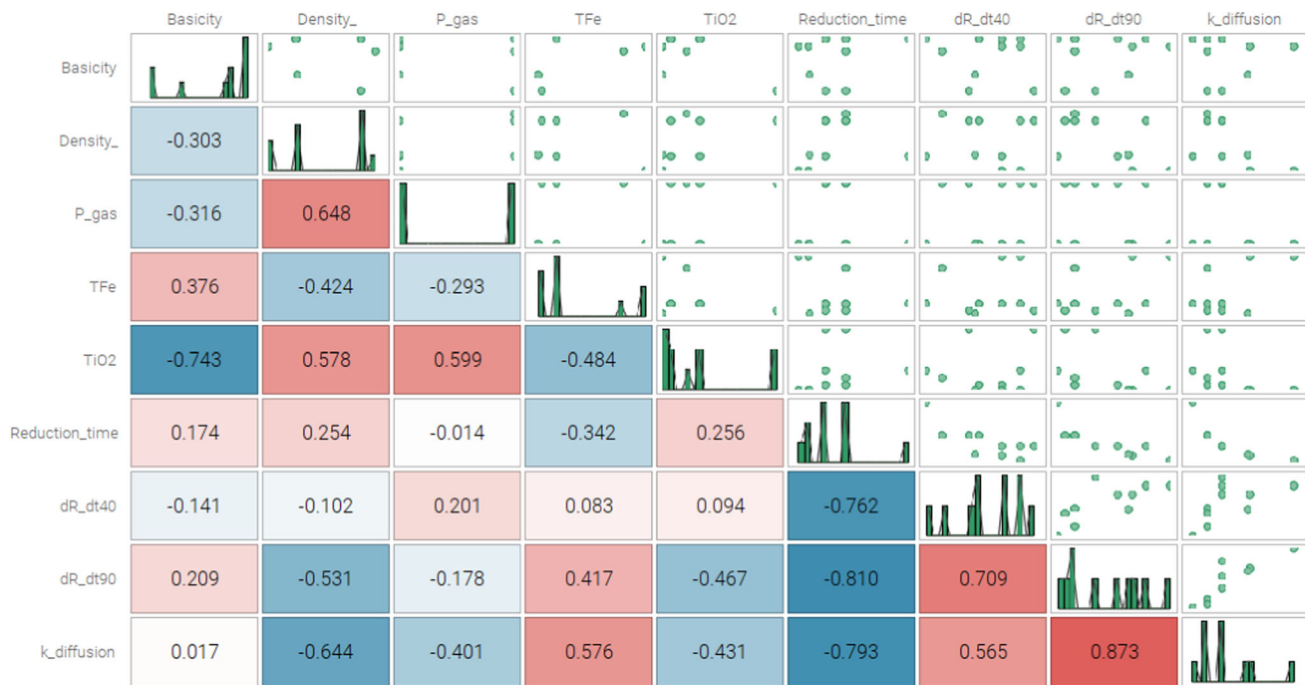
	Basicity	Density_	P_gas	TFe	TiO2	Reduction_time	dR_dt40	dR_dt90	k_diffusion
Basicity									
Density_	-0.303								
P_gas	-0.316	0.648							
TFe	0.376	-0.424	-0.293						
TiO2	-0.743	0.578	0.599	-0.484					
Reduction_time	0.174	0.254	-0.014	-0.342	0.256				
dR_dt40	-0.141	-0.102	0.201	0.083	0.094	-0.762			
dR_dt90	0.209	-0.531	-0.178	0.417	-0.467	-0.810	0.709		
k_diffusion	0.017	-0.644	-0.401	0.576	-0.431	-0.793	0.565	0.873	

Fig. 12—Scatter matrix of the Iron oxide direct reduction of the VALE pellets in the presence of 100 pct H_2 as the reducing gas at 900 C.

TiO_2 is a key parameter influencing the reduction rate, time, and diffusion kinetics. Under a CO atmosphere at 1000 °C, a nuanced transition range for the TiO_2 effect is observed, with an optimal range between 1 and 1.5 pct TiO_2 identified. Above this threshold, a counterintuitive trend emerges, highlighting the complicated nature of the influence of TiO_2 on the direct reduction process. The introduction of H_2 into the CO atmosphere not only extends this transition range, but also significantly accelerates the reduction rate and exceeds the effectiveness of a pure CO atmosphere. In a reducing H_2 atmosphere alone, the influence of TiO_2 becomes more sensitive, with an optimum point identified at 0.5 pct TiO_2, indicating a complex interplay with the basicity index and the reducing atmosphere. Temperature variations further emphasize the sensitivity of the TiO_2 effect, with a higher TiO_2 content correlating with a longer reduction time in a 100 pct H_2 atmosphere at 900 °C, highlighting the temperature dependence. The role of TiO_2 is significantly influenced by temperature fluctuations, which have a direct effect on the thermodynamic stability and kinetic behavior of titanium-containing compounds such as ilmenite ($FeTiO_3$) and pseudobrookite (Fe_2TiO_5). From a thermodynamic point of view, the stability of these titanium-containing phases can be described quantitatively by changes in Gibbs free energy with temperature. As the temperature increases, the Gibbs free energy for the formation of these phases generally decreases, indicating increased stability and a shift in equilibrium in favor of the formation of these compounds. This shift may inhibit the reduction process as these stable titanium oxides are less easily reduced compared to iron oxides. On the other hand, from a kinetic point of view, the effect of temperature on the reaction rates with TiO_2 is critical.

The activation energies of the reactions that lead to the formation and reduction of $FeTiO_3$ and Fe_2TiO_5 determine the temperature sensitivity of these processes. Higher temperatures generally lower the activation barriers and accelerate the kinetics of these reactions. This can lead to a faster formation of titanium-containing phases in the initial stages of heating, followed by an increase in their reduction rate at higher temperatures. In addition, the diffusion rates of titanium ions and oxygen within the pellet matrix are also enhanced at higher temperatures, allowing faster transport of reactants and products to and from the reaction sites. This improved diffusion is critical to maintaining the efficiency of the reduction process, particularly in dense pellet structures where diffusion pathways can be significantly impeded. The multi-criteria optimization analysis confirms the nuanced effects of TiO_2 content on the reduction process in different atmospheres and highlights the need for a nuanced understanding of the role of TiO_2 in the optimization of iron oxide reduction processes.

Improving the conditions for reduction kinetics with TiO_2 can lead to an increase in the final degree of reduction. This is because the reduction kinetics directly influence the rate at which iron oxide is converted to metallic iron. By enhancing the conditions for the reduction kinetics with TiO_2, the process of converting iron oxide into metallic iron is accelerated, resulting in a higher final degree of reduction. This is in line with the results of the present work, which highlights the concentration-dependent behavior of TiO_2 and its optimal range in which a neutral or positive effect on the reduction kinetics is observed. Thus, by improving the conditions for the reduction kinetics with TiO_2, the efficiency of the reduction process is increased, which

ultimately leads to a higher final reduction degree. Research results indicate that TiO_2 acts as a catalyst and improves the reduction kinetics by forming active sites.[11,27,42] However, increased TiO_2 concentrations can cause problems, such as the formation of stable oxide phases that hinder the reduction process.[42] Understanding the complicated role of TiO_2 is crucial for improving the reduction conditions. Figures 13 and 14 illustrate the complexity of TiO_2 behavior and highlight its sensitivity to parameters such as the reducing atmosphere, temperature, pressure, and the presence of other non-ferrous oxides. The reduction rate shows different responses to different TiO_2 concentrations under different reducing atmospheres. In Figures 3 and 4, the parameters dR/dt40 and dR/dt90 under 100 pct CO initially show a decrease with increasing TiO_2 content up to 1 pct before showing an upward trend. This is due to the significant solubility of TiO_2 in hematite and magnetite, which enhances the catalytic effect and influences oxygen diffusion. However, an excess of TiO_2 can lead to the formation of micropores or voids, which has a negative effect on the reduction rate. The optimum reduction rate is observed at TiO_2 concentrations below 0.5 pct. In contrast, at 100 pct H_2 with TiO_2, the reduction rate increases up to 0.5 pct and then decreases, possibly due to the fact that TiO_2 is less reducible than iron oxides and dilutes the concentration of reducible iron oxides (example of reduction curve is provided in Figure 13).

In addition, TiO_2 plays a crucial role in preventing the reoxidation of reduced iron by reacting with residual oxygen in the system.[7] This prevention is crucial for maintaining the integrity of the reduced iron and ensures that the benefits of the reduction process are not compromised.[9] In addition, TiO_2 contributes to an accelerated direct reduction rate of iron oxide pellets by facilitating the formation of a liquid phase during the reduction process.[43,44] This liquid phase serves as a conduit that supports the transportation of the reducing gases to the surface of the iron oxide particles where the crucial reduction reactions take place. The promotion of
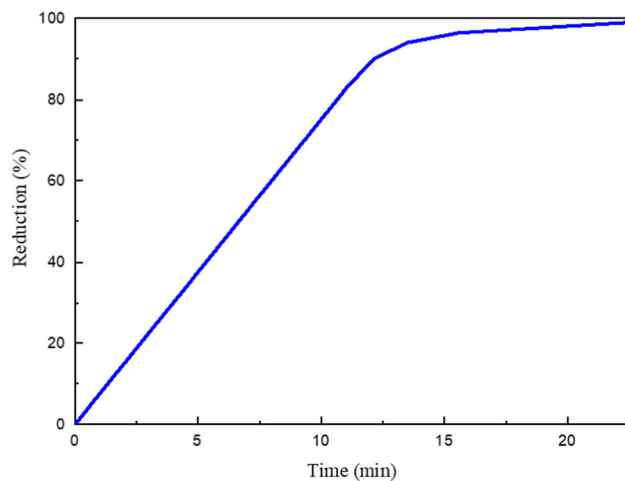
a liquid phase by TiO_2 demonstrates its versatile role in facilitating efficient gas transport, a factor that is essential for sustainable reduction reactions.[11] In fact, the presence of TiO_2 oxide contributes to an increase in the surface area of the iron oxide particles, leading to an increase in porosity of about 80 pct, as shown in Figure 16 (Additional tomography pictures of the unreduced and reduced pellets are provided in Figures S1 through S12 of electronic Supplementary material). This increase in size is attributed to the creation of additional active sites due to the increased surface area, which favors a stronger interaction with the reducing gas.[27] The basicity index is considered one of the influential parameters for the reduction behavior of iron ore.[2,4] Figures 10, 11, and 12 show its strong negative influence on the reduction parameters under a reducing gas of 100 pct CO, although this effect diminishes with the addition of 50 pct H_2. In a 100 pct CO atmosphere at 1000 °C and a high basicity index (above 2.5), the time to reduction decreases slightly but remains relatively high, possibly due to the formation of a basic slag that facilitates the reduction of the iron ore but is less effective at higher TiO_2 content. The higher H_2 concentration at elevated pressure probably improves the reaction kinetics as TiO_2 is not easily reduced by H_2, which could hinder the reduction of iron oxides. CaO, which has a significant influence on the reduction behavior, acts through reactivity and catalytic effects. Studies indicate that CaO increases the reduction rate by facilitating the formation of a liquid phase, promoting the migration of iron particles and accelerating the reduction kinetics.[4,45,46]

In addition, the addition of CaO reduces the solubility of FeO in the slag phase and inhibits the formation of fayalite.[47] The presence of CaO leads to a higher porous structure, which improves the reducibility of iron oxide.[4,48] As a fluxing agent, CaO lowers the melting point of gangue and thus supports the formation of a liquid phase that favors the reduction process. SiO_2 influences the reduction behavior by affecting the viscosity of the slag and the formation of the liquid phase. A higher SiO_2 content increases the viscosity of the slag and hinders the movement of gas bubbles and iron particles. In addition, a higher SiO_2 content leads to the formation of the Fe_2SiO_4 phase, which significantly hinders the CO reduction of FeO compacts.[49] SiO_2 also plays a role in the formation of stable phases that influence the overall reduction kinetics. The formation of liquid slag phases at elevated temperatures promotes efficient mass transfer mechanisms and improves the kinetics of the reduction process.[50–52]

An increase in basicity up to the range of 1.5 to 2 has a positive effect on the reduction rate (dR/st40 and dR/dt90), followed by a subsequent decrease. These results are consistent with previous studies.[4,53,54] For example, Mishra *et al.*[4] observed a significant increase in reduction with the addition of CaO, which peaked at a certain threshold (4 wt pct). Beyond this threshold, however, the degree of reduction decreased with a further increase in the CaO content of the pellets. They also investigated the effects of basicity and found that the highest levels of reduction and metallization were
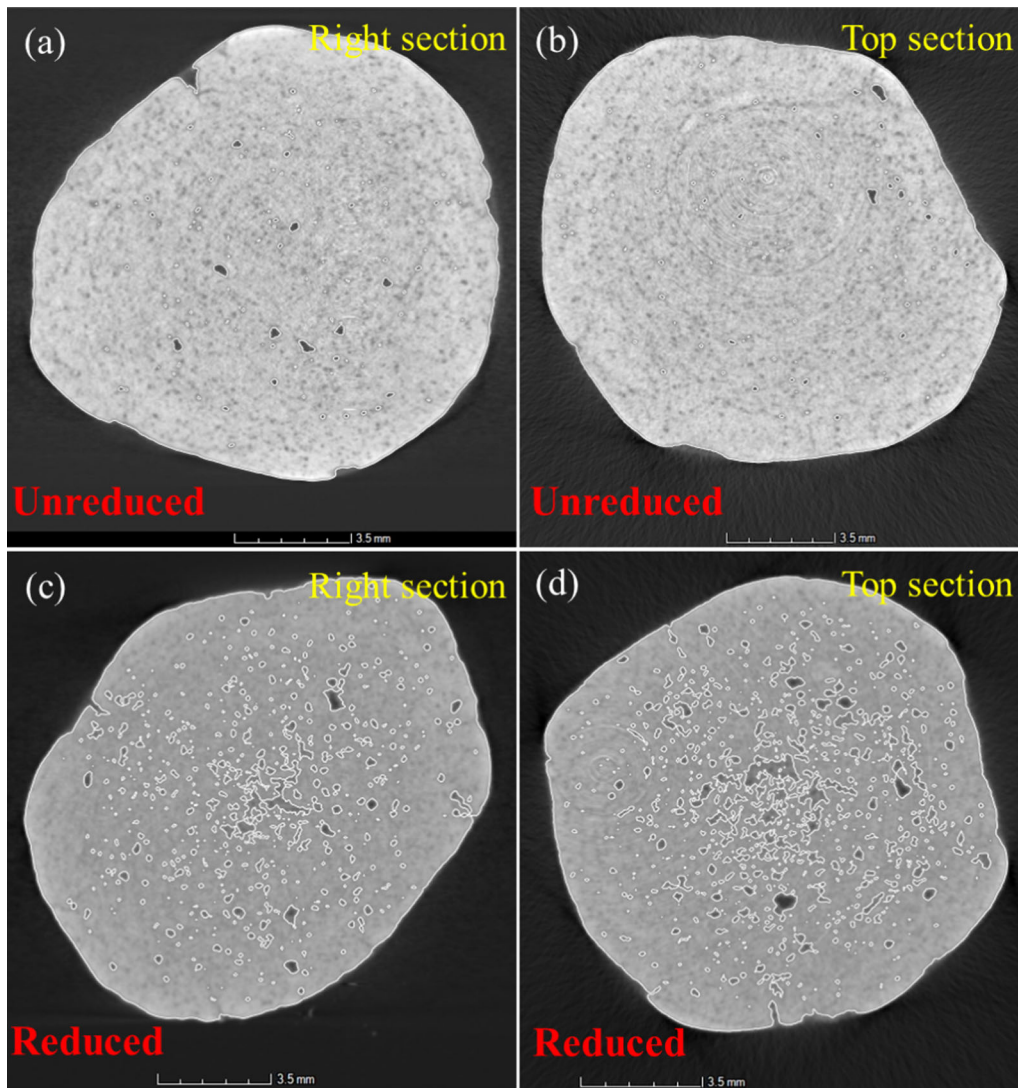

Fig. 13—Reduction curve for the pellets (in bold in Table I) at 950 °C and 1 bar in H_2 atmosphere.

Fig. 14—The X-ray tomography images of the (*a*, *b*) unreduced, and (*c*, *d*) reduced pellets in 100 pct H$_2$ as reducing gas. The porosity value for unreduced pellets was about 35 pct and increased by about 63 pct for the reduced one. The pellet composition as an example is referred to the one in bold in Table I. The whole database is visible as supplementary material.

achieved at a basicity index of 1.6. This trend suggests that there is an optimal basicity range for maximizing reduction efficiency. In addition, the mechanism behind the positive influence of basicity on the reduction rate has been investigated in the literature. Increased porosity of the pellets, which usually occurs in the presence of CaO, contributes to an increased reduction rate. Studies suggest that the formation of acicular calcium ferrite and lattice transformations caused by lattice distortion in the presence of CaO lead to increased porosity in the pellet structure. This improves diffusion in the product layers, leading to an overall increase in the reduction rate. Higher basicity also promotes the formation of a more basic slag with a lower melting point, facilitating the formation of a liquid phase, which is crucial for the reduction of iron oxide. This liquid phase is essential for the mobility of iron particles and gas bubbles and contributes to faster reduction kinetics.[4,54–56]

CO reacts with iron oxide to form CO$_2$ and metallic iron. However, the presence of TiO$_2$ appears to hinder this reaction, possibly due to the formation of stable Ti compounds that are not easily reduced by CO. While the basic slag may enhance the reduction process, its effectiveness could be compromised at higher TiO$_2$ content. A higher TiO$_2$ content could lead to the formation of stable compounds with the slag components and change the properties of the slag. These interactions may affect the ability of the slag to efficiently support the reduction of the iron ore. TiO$_2$ has a significant influence on the viscosity and melting properties of the slag. With a higher TiO$_2$ content, the composition and properties of the slag change in a way that reduces its effectiveness in promoting rapid reduction, resulting in lower reduction rates. Longer reduction times at lower total iron content, especially below about 64 pct TFe, can be explained by the principle that lower iron content naturally leads to longer reduction

times due to the lower amounts of reducible material. A lower total iron content means that less iron is available for reduction, resulting in a smaller volume of material going through the reduction reaction. The rate at which iron oxide is reduced to metallic iron depends on the availability of reducible material and the kinetics of the reduction reactions. With a lower total iron content, less material is available for oxygen removal and the reduction reactions proceed more slowly due to the limited amount of iron available for the reaction. The decrease in diffusion coefficient with increasing reducing gas pressure suggests that the reaction may be less diffusion limited at high pressure and more controlled by the surface reaction. This suggests that the process at high pressures could benefit from optimizing the surface properties of the pellets for better reactivity rather than focusing only on the diffusion characteristics. The CO atmosphere promotes the Boudouard reaction, in which CO reduces iron oxides to iron.[57] However, a higher TiO_2 content could inhibit this reaction as TiO_2 is not as easily reduced by CO, leading to a decrease in the diffusion coefficient. In addition, a higher basicity index is more likely to lead to the formation of a more liquid slag, possibly hindering gas diffusion through the pellet and thus lowering the diffusion coefficient. H_2, with its smaller molecular size and higher reactivity, has a higher diffusion coefficient than CO under these conditions, possibly explaining the higher diffusion coefficients in this syngas mixture. Optimal diffusion seems to occur at a moderate basicity index, suggesting that while some slag formation is beneficial to the reduction process, excess could hinder gas diffusion.

Therefore, it can be concluded that the presence of TiO_2, which does not contribute to reduction in a 100 pct H_2 atmosphere, is due to the phenomenon of the water-gas shift reaction. When TiO_2 is present, it can act as a catalyst for the water-gas shift reaction, which leads to the production of additional water vapor from the H_2 and CO present. This water vapor can then react with the iron oxide, leading to the formation of more stable iron hydroxides that hinder the reduction process in a 100 pct H_2 atmosphere.[19,58] On the other hand, in the presence of TiO_2, the introduction of H_2 into the reducing atmosphere controlled by CO can increase the transition area and accelerate the reduction rate due to the synergistic interaction of CO and H_2. CO has a higher reactivity with iron oxide, and its introduction into the atmosphere can create a favorable environment for the initial stages of reduction. The subsequent introduction of H_2 complements this process by further promoting the reduction of iron oxide, resulting in an extended transition region and an accelerated reduction rate.[59–61] Compared to existing data and theories, our results are consistent with the observations of Mohanty et al.[4], who reported an increase in reduction efficiency upon addition of CaO, which peaked at 4 wt pct. However, our study provides new insights by investigating the nuanced effects of TiO_2 content on the reduction process and reveals a transition range between 1 and 1.5 pct TiO_2 with optimal effects on the reduction kinetics. Our research contributes to this understanding by demonstrating the interplay of TiO_2 and basicity

index in different reducing atmospheres and temperatures. Moreover, the influence of TiO_2 on the reduction process mirrors the catalytic effects reported in previous studies.[4,53,54] Beyond this optimal value, Paananen et al.[11] have shown that as the TiO_2 content in solid solution in magnetite increases, the oxidation rate accelerates, which in turn negatively affects the reduction strength of the sinter and the reducibility of the pellets. Our results extend this knowledge by demonstrating the concentration-dependent behavior of TiO_2 and its role in the formation of stable oxide phases that can hinder the reduction process.[47] In addition, the observed increase in porosity due to TiO_2 addition is consistent with studies reporting increased porosity of pellets in the presence of CaO, which contributes to an increased reduction rate.[4,48] These comparisons emphasize the importance of our results in the broader context of the existing literature on iron oxide reduction processes and provide a more comprehensive understanding of the multifaceted role of TiO_2 in this complex system.

Possible mechanisms of the influence of TiO_2 under different reducing atmospheres can be described as follows: First, TiO_2 changes the viscosity and melting behavior of the slag during the reduction process, which influence mass transfer and chemical reactions within the pellet matrix. TiO_2 changes the physical properties of the slag formed during the reduction process. A higher TiO_2 content usually increases the viscosity of the slag, which can hinder the movement of reduction gasses and molten iron within the pellet matrix. This increase in viscosity can slow down the rate of reduction as it hinders the mass transfer processes required for efficient reduction. In addition, the presence of TiO_2 can affect the melting behavior of slag components, potentially increasing the melting point. This change could result in the slag being less liquid at the operating temperature, affecting the coalescence of iron grains and the movement of gas bubbles, which are critical for effective reduction.

Second, in hydrogen and CO atmospheres, TiO_2 potentially catalyzes key reactions such as the water-gas shift and Boudouard reactions, affecting local gas composition and reaction kinetics. In a reducing atmosphere consisting predominantly of hydrogen, TiO_2 could act differently than in a CO-containing atmosphere. TiO_2 can potentially catalyze the water-gas shift reaction, where CO and water vapor react to form CO2 and more H_2, affecting the local H_2/CO ratio and thus the reduction dynamics. Furthermore, in CO2- rich atmospheres, TiO_2 could influence the Boudouard reaction (CO_2 + C = 2CO), where its catalytic properties could either enhance or inhibit the reaction depending on the specific conditions and the interaction of TiO_2 with other elements in the slag. Then, the addition of TiO_2 can change the phase formation and sintering behavior and affect the porosity, permeability, and structural integrity of the iron oxide pellets. TiO_2 leads to the formation of stable titanium-containing compounds within the iron matrix or slag, such as Fe_2TiO_5 or $FeTiO_3$. These phases are generally more resistant to reduction and could therefore hinder the

overall kinetics of reduction. Furthermore, the addition of TiO_2 could change the porosity of the pellet by affecting the sintering behavior during pellet formation. Higher porosity generally improves reducibility by increasing the surface area accessible to reducing gasses. However, the formation of dense, titanium-rich phases could reduce the effective porosity.

In a blast furnace, the presence of TiO_2 could lead to faster reduction rates, reduce coke consumption, and improve the overall energy efficiency of the furnace. In fact, TiO_2 is a known component of slag and influences its viscosity and melting behavior. A high TiO_2 content can increase the viscosity of the slag, making slag tapping more difficult and possibly leading to a build-up in the furnace and irregularities in the internal furnace pressure. The altered composition of the slag can also affect the removal of sulfur and other impurities. Depending on the concentration and distribution of TiO_2 in the pellets, this can even affect the longevity and performance of the refractories used in the blast furnace. In other words, TiO_2 in the slag phase can interact with the refractories and accelerate wear and degradation, which could require more frequent maintenance and affect the overall stability of the blast furnace operation. In addition, the presence of TiO_2 could affect the solubility of carbon in the molten iron, which would affect the final carbon content and mechanical properties of the iron produced. While TiO_2-enriched pellets are promising to improve the reduction process, their integration into blast furnace operations, especially in the production of iron grades that require special mechanical properties, should be approached with caution.

Finally, TiO_2 affects the diffusion of gasses and solids within the pellets by changing the surface properties and internal structures, thus affecting the overall reduction rates and efficiency. The presence of TiO_2 could alter the surface properties of iron oxides and affect the adsorption and reaction kinetics of reducing gasses on the pellet surface. Depending on the nature of the surface changes induced by TiO_2, this could either increase or slow down the rate of reduction. If TiO_2 leads to the formation of more compact and less porous structures, the diffusion of ions and electrons through the pellet could be hindered, affecting the overall reduction rate. Nevertheless, additional experimental, namely, advanced microscopic and spectroscopic analyses and theoretical studies such as kinetic modeling should be considered.

V. CONCLUSION

In conclusion, this study provides a comprehensive analysis of the influence of TiO_2 on the reduction of iron oxide pellets under different conditions of temperature, pressure, and gas composition. Our results indicate that while higher concentrations of TiO_2 typically hinder the reduction process, there is a favorable concentration window of 1 to 1.5 pct TiO_2 in which the effect on

reduction kinetics and diffusion coefficients becomes neutral or positive. This finding is of crucial importance for the optimization of industrial reduction processes.

The most important results of our research include

1. The combination of CO and H_2 gasses at a temperature of 1000 °C and increased pressure dramatically improves the reduction process. This optimal condition has been shown to reduce the time to complete reduction by up to 20 pct compared to conditions without this gas mixture. Such efficiency is crucial for improving throughput in industrial applications.
2. Temperature plays a crucial role. Our experiments show that increasing the temperature from 900 °C to 1000 °C can shorten the reduction time by about 15 pct at different TiO_2 concentrations. This underlines the importance of temperature management in industrial furnaces to maximize the reduction rate.
3. The effect of pressure was quantitatively significant. Increasing the pressure from 1 atm to 5 atm led to an improvement in reaction rates and a 25 pct reduction in the time to complete reduction. This underlines the potential of pressure optimization in the industry to accelerate the reduction process.
4. This study also confirms the positive correlation between total iron content and reduction performance. Increasing the TFe content from 85 pct to 95 pct was associated with a 10 pct improvement in the reduction rate and a corresponding reduction in the time to complete reduction. This suggests that the selection of higher quality iron materials could be a strategic approach to improve the efficiency of the reduction process in industrial applications.

These results provide actionable insights for the iron and steel producing industry. The results suggest that careful manipulation of TiO_2 content together with strategic control of operating parameters such as temperature, pressure, and gas composition can lead to significant improvements in the efficiency and cost-effectiveness of the reduction process. The findings of this research not only contribute to the academic understanding of the dynamics of iron oxide reduction, but also provide practical guidance for improving the operation of industrial furnaces to achieve more sustainable and economically viable production results.

CONFLICT OF INTEREST

The authors declare no conflict of interest

FUNDING

OPEN ACCESS

SUPPLEMENTARY INFORMATION

The online version contains supplementary material available at https://doi.org/10.1007/s11663-024-03168-1.

REFERENCES

1. H. Zhong, D. Er, and L. Wen: *Appl. Surf. Sci.*, 2017, vol. 399, pp. 630–37.
2. J. Jian-tao, X.-T. Jiang, G.-Q. Zhao, and Lu. Feng-lin: *Metall. Res. Technol.*, 2023, vol. 120, p. 306.
3. Z. Wang: *Acad. J. Sci. Technol.*, 2022, vol. 4, pp. 108–11.
4. M. Kumar Mohanty, S. Mishra, B. Mishra, and S. Sarkar: *Arab. J. Sci. Eng.*, 2018, vol. 43, pp. 5989–98.
5. B. Sadeghi, P. Cavaliere, M. Bayat, et al.: *Int. J. Hydrogen Energy*, 2024, vol. 69, pp. 586–607.
6. T.S. Paananen and K. Kinnunen: *Steel Res. Int.*, 2009, vol. 80, p. 408.
7. J.T. Ju, Q. Li, X. Xing, X. Jiang, G. Zhao, and F. Lu: *Metall. Res. Technol.* 2023.
8. H. Park and V. Sahajwalla: *Metall. Mater. Trans. B.*, 2013, vol. 44, pp. 1379–89.
9. P. Cavaliere, L. Dijon, A. Laska, and D. Koszelow: *Int. J. Hydrogen Energy*, 2024, vol. 49, pp. 1235–54.
10. A.N. Dmitriev, R.V. Alektorov, G.Y. Vitkina, S.A. Petrova, and Y.A. Chesnokov: *Defect Diffusion Forum Trans. Tech. Publ.*, 2020, vol. 2020, pp. 176–85.
11. T.P. and K. Kinnunen: *Steel Res. Int.* 2009, vol. 80, pp. 408–14.
12. J. Tang, M.-S. Chu, F. Li, Y.-T. Tang, Z.-G. Liu, and X.-X. Xue: *Int. J. Miner. Metall. Mater.*, 2015, vol. 22, pp. 562–72.
13. Y. Weng, X. Sun, M. Gou, B. Liu, S. Yang, and Z. Deng: *Trans. Comput. Sci. Res. Intell. Syst. Res.*, 2023, vol. 2, pp. 62–6.
14. H. Song, S. Han, Y. Li, J. Cheng, and D. Xu: *Yingyong Lixue Xuebao*, 2011, vol. 28, pp. 39–43.
15. P. Cavaliere: *Clean Ironmaking and Steelmaking Processes: Efficient Technologies for Greenhouse Emissions Abatement*, Springer, Berlin, 2019, pp. 1–37.
16. P. Cavaliere, A. Perrone, A. Silvello, P. Stagnoli, and P. Duarte: *Metals*, 2022, vol. 12, p. 203.
17. M. Shahabuddin, G. Brooks, and M.A. Rhamdhani: *J. Clean. Prod.*, 2023, vol. 395, p. 136391.
18. M. Aeppli, A. Voegelin, C.A. Gorski, T.B. Hofstetter, and M. Sander: *Environ. Sci. Technol.*, 2018, vol. 52, pp. 560–70.
19. S. Bagheri, N.M. Julkapli, and S.B. AbdHamid: *Sci. World J.*, 2014, vol. 2014, p. 727496.
20. P.E. Duarte Leobardo Chapa: HYL technology from HYLSA-MEX, CVRD seminar. 2021.
21 H.P. Pimenta and V. Seshadri: *Ironmaking Steelmaking*, 2002, vol. 29, pp. 175–9.
22. N.J. Bristow and C.E. Loo: *ISIJ Int.*, 1992, vol. 32, pp. 819–28.
23. Y. Jianwen, H. Nan, H. Xiao, P. Gao, and Y. Sun: *Powder Technol.*, 2021, vol. 385, pp. 83–91.
24. Y. Jianwen, Ou. Yang, Y. Sun, Y. Li, and Y. Han: *Powder Technol.*, 2022, vol. 402, p. 117340.
25. A. Zulkania, R. Rochmadi, M. Hidayat, and R.B. Cahyono: *Energies*, 2021, vol. 15, p. 137.
26. W. Jian, S.-P. Wang, H.-X. Zhang, and F.-Q. Bai: *Inorg. Chem. Front.*, 2019, vol. 6, pp. 2660–6.
27. S. Bonanni, K. Aït-Mansour, W. Harbich, and H. Brune: *J. Am. Chem. Soc.*, 2012, vol. 134, pp. 3445–50.
28. W. Zhang, Y. Li, S. Zhu, and F. Wang: *Chem. Phys. Lett.*, 2003, vol. 373, pp. 333–7.
29. A.D. Yewale, P.V. Kherdekar, and D. Bhatia: *Chem. Eng. Sci.*, 2022, vol. 249, p. 117281.
30. F. Irfan, M.U. Tanveer, M.A. Moiz, S.W. Husain, and M. Ramzan: *Eur. Phys. J. B*, 2022, vol. 95, p. 184.
31. J. Fang, Z. Pang, X. Xing, and R. Xu: *Materials*, 2020, vol. 14, p. 1.
32. Y. Li, L. Liu, M. Guo, and M. Zhang: *J. Environ. Sci. (China)*, 2016, vol. 47, pp. 14–22.
33. C. Scharm, F. Küster, M. Laabs, Q. Huang, O. Volkova, M. Reinmöller, S. Guhl, and B. Meyer: *Miner. Eng.*, 2022, vol. 180, p. 107459.
34. E. Hjortsberg, F. Forsberg, G. Gustafsson, and E. Rutqvist: *Ironmaking Steelmaking*, 2013, vol. 40, pp. 399–406.
35. L.C. Bam, J.A. Miller, M. Becker, and I.J. Basson. *Miner. Eng.*, 2019, vol. 131, pp. 206–15.
36. P. Cavaliere, A. Perrone, L. Dijon, A. Laska, and D. Koszelow: *Int. J. Hydrog. Energy*, 2024, vol. 49, pp. 1444–60.
37. P. Cavaliere, A. Perrone, and D. Marsano: *Ironmaking Steelmaking*, 2023, vol. 50, pp. 1045–64.
38. P. Cavaliere, A. Perrone, and D. Marsano: *Powder Technol.*, 2023, vol. 426, p. 118650.
39. P. Cavaliere, A. Perrone, and A. Silvello: *J. Manuf. Process.*, 2015, vol. 17, pp. 9–27.
40. P Cavaliere and ANGELO Perrone: *Ironmaking Steelmaking* 2013, vol. 40, pp. 9–24.
41. Y. Man and J. Feng: *Powder Technol.*, 2016, vol. 301, pp. 674–8.
42. E. Park and O. Ostrovski: *ISIJ Int.*, 2003, vol. 43, pp. 1316–25.
43. Y. Chai, Y. Fan, Z. Li, Wu. Jiayi, Y. Zhang, Y. Wang: *Guo Ping Luo, and Shengli An: ACS Omega*, 2022, vol. 7, pp. 7759–68.
44. O.B. Skibelid, S.O. Velle, F. Vollan, C. Van der Eijk, A. Hoseinpur-Kermani, and J. Safarian: *Materials (Basel, Switzerland)* 2022, vol. 15.
45. H.T. Wang and H.Y. Sohn: *Ironmaking Steelmaking*, 2011, vol. 38, pp. 447–52.
46. Z.-L. Zhao, H.-Q. Tang, and Z.-C. Guo: *J. Iron Steel Res. Int.*, 2013, vol. 20, pp. 16–24.
47. S. Prakash, M.C. Goswami, A.K.S. Mahapatra, and K.C. Ghosh: *Ironmaking Steelmaking*, 2000, vol. 27, pp. 194–201.
48. P.K. Strangway and H.U. Ross: *Can. Metall. Q.*, 1965, vol. 4, pp. 97–111.
49. K. Jabbour and N. El Hassan: *Chem. Eng. Sci.*, 2022, vol. 252, p. 117297.
50. J. Park, S. Sridhar, and R.J. Fruehan: *Metall. Mater. Trans. B*, 2014, vol. 45B, pp. 1380–8.
51. R. Zeng, N. Wang, and W. Li: *Powder Technol.* 2021.
52. F. Ding, A. Zhang, M. Liu, X. Guo, and C.H. Song: *RSC Adv.*, 2014, vol. 4, pp. 8930–8.
53. S.-M. Jung: *Metall. Mater. Trans. B.*, 2015, vol. 46B, pp. 1162–74.
54. A. Basumallick: *ISIJ Int.*, 1995, vol. 35, pp. 1050–3.
55. L.H. Zhou and F.H. Zeng: *Adv. Mater. Res.*, 2010, vol. 97, pp. 465–70.

56. K.-I. Ohno, H. Konishi, T. Watanabe, S. Ishihara, S. Natsui, T. Maeda, and K. Kunitomo: *ISIJ Int.*, 2020, vol. 60, pp. 1520–7.
57. K. Mondal, H. Lorethova, E. Hippo, T. Wiltowski, and S.B. Lalvani: *Fuel Process. Technol.*, 2004, vol. 86, pp. 33–47.
58. R. Bouarab, S. Bennici, C. Mirodatos, and A. Auroux: 2014.
59. S. Li, H. Zhang, J. Nie, R. Dewil, J. Baeyens, and Y. Deng: *Sustainability*, 2021, vol. 13, p. 8866.
60. L. Qing, Z. Xiaofang, Y. Zhang, Z.Z. Fang, S. Zheng, P. Sun, Y. Xia, P. Li, Y. Zhang, and X. Zou: *Chem. Eng. Sci.*, 2019, vol. 195, pp. 484–93.
61. T. Mizuno, K. Adachi, K. Ohta, and A. Saji: *J. Photochem. Photobiol. A*, 1996, vol. 98, pp. 87–90.